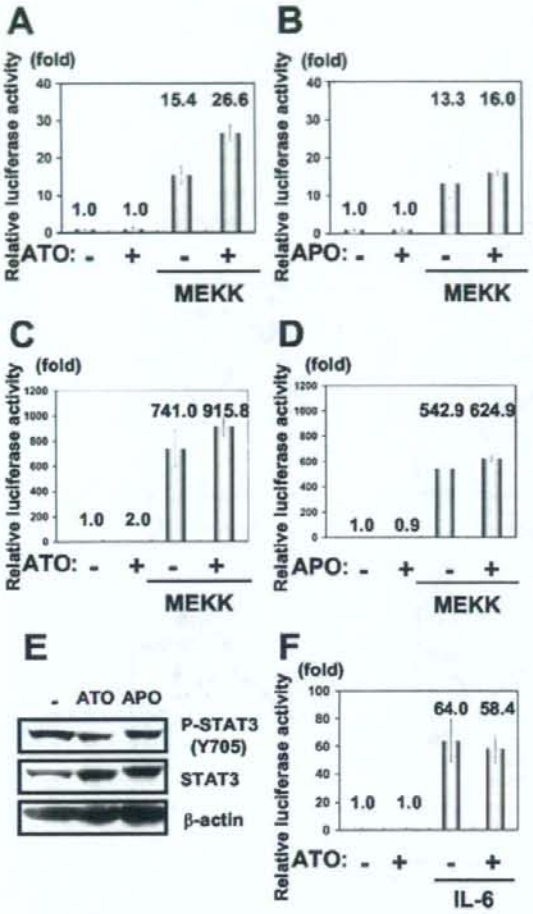

FIG. 5. Effect of ATO on the stress-signaling pathways. (A and B) Effect of ATO or APO on the NF-κB signaling pathway. O cells were transfected with 100 ng of reporter plasmid, pNF-κB-Luc, and/or 100 ng of pFC-MEKK (Stratagene, La Jolla, CA). Cells were treated with either 1 μM ATO (A) or 1 μM APO (B), and an FL assay was performed 24 h later. The results shown are means from three independent experiments. The relative FL activity is shown. (C and D) Effect of ATO or APO on the AP-1 signaling pathway. O cells were transfected with 100 ng of pAP-1-Luc and/or 100 ng of pFC-MEKK (Stratagene). Cells were treated with either 1 μM ATO (C) or 1 μM APO (D), and an FL assay was performed 24 h later as described for panels A and B. (E) Effect of ATO on the phosphorylation level of STAT3 at tyrosine 705. The results of Western blot analysis of cellular lysates with anti-phospho-STAT3 (Tyr705), anti-STAT3, or anti-β-actin antibody in O cells treated with either 1 μM ATO or 1 μM APO for 24 h are shown. (F) Effect of ATO on the STAT3 signaling pathway. O cells were transfected with 100 ng of STAT3 reporter APRE-Luc (41) (STAT3-Luc, a generous gift from T. Hirano, Osaka University, Japan). Cells were treated with 1 μM ATO for 19 h and then stimulated with 100 ng/ml of interleukin-6 for 5 h, and an FL assay was performed as described for panels A and B.

level was suppressed by about 30% compared with that of the control cells, and this occurred without cell toxicity (data not shown). However, consistent with previous reports in which ATO-induced apoptosis was enhanced by BSO (14, 20, 33), most of the cells died, possibly through apoptosis, when the OR6 cells were cotreated with 1 μM ATO and 1 μM BSO for 72 h (data not shown), suggesting that ATO and BSO synergistically generate ROS and deplete glutathione, resulting in induction of oxidative damage. Taken together, these results suggest that ATO may inhibit the HCV RNA replication by modulating the glutathione redox system and oxidative stress.

DISCUSSION

ATO has been reported to affect multiple biological functions, such as PML-NB formation, apoptosis, differentiation, stress response, and viral infection (38). Indeed, ATO has been shown to increase retroviral infectivity, including infectivity of HIV-1, HIV-2, feline immunodeficiency virus, simian immunodeficiency virus from rhesus macaques, and murine leukemia virus, although the mechanisms responsible for these changes are not well understood (5, 6, 32, 44, 47, 50, 57). PML, which is involved in host antiviral defenses, is required for the formation of the PML-NB, which is often disrupted or sequestered in the cytoplasm by infection with DNA or RNA viruses (17). The fact that ATO promotes the degradation of PML and alters the morphology or distribution of PML-NBs suggests that ATO enhances HIV-1 infection by antagonizing an antiviral activity associated with PML. In fact, HIV-1 infection has been reported to alter PML localization (57), although others have failed to confirm this finding (5). Furthermore, Berthoux et al. demonstrated that ATO stimulated retroviral reverse transcription (5). Moreover, ATO has been shown to have an inhibitory effect on host restriction factors, such as TRIM5α, Ref1, and Lv1, in a cell type-dependent manner (5, 6, 32, 44, 47, 50). In contrast, we have demonstrated that ATO strongly inhibited genome-length HCV RNA replication without cell toxicity (Fig. 1A and 2A). In addition, we observed the cytoplasmic translocation of PML in the HCV RNA-replicating O cells after the treatment with ATO (Fig. 4A). However, PML was dispensable for the anti-HCV activity of ATO as well as HCV RNA replication (Fig. 4E). In this regard, it is worth noting the recent report by Herzer et al. that the HCV core protein interacts with PML isoform IV and abrogates the PML function (22). Thus, PML may be involved in the HCV life cycle. In any case, the sensitivity to ATO and the cellular target of ATO seem to be different between HCV and HIV-1.

HCV infection has been shown to cause a state of chronic oxidative stress like that seen in chronic hepatitis C, which may contribute to fibrosis and carcinogenesis in the liver (16, 18, 40). In particular, HCV replication has been associated with the endoplasmic reticulum (ER), where HCV causes ER stress. Indeed, HCV NS5A and core, the ER-associated proteins, have been reported to trigger ER stress (4, 55). Therefore, HCV infection causes production of ROS and lowering of mitochondrial transmembrane potential through calcium signaling (4, 36). Among the HCV proteins, core, E1, NS3, and NS5A have been shown to be potent ROS inducers, and these HCV proteins also alter intracellular calcium levels and induce oxidative stress, thereby inducing DNA damage, and constitu-

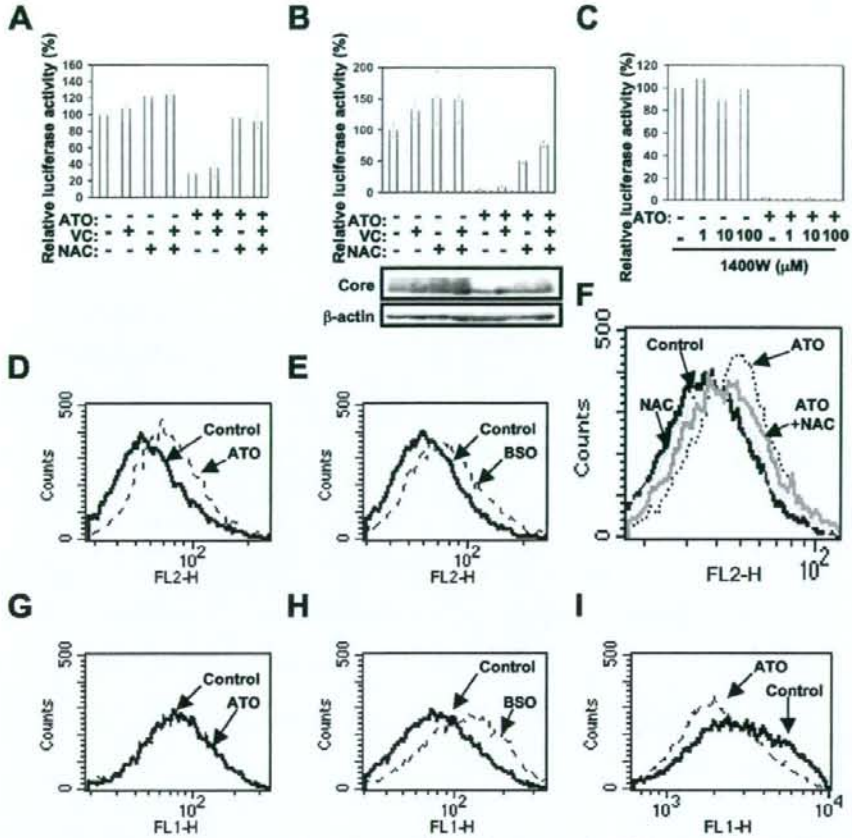

FIG. 6. The anti-HCV activity of ATO is associated with the glutathione redox system and oxidative stress. (A and B) The anti-HCV activity of ATO is eliminated by treatment with the antioxidant NAC. OR6 cells were treated with 1 μM ATO alone and in combination with 100 μM vitamin C (VC), with or without 10 mM NAC, for 24 h (A) or 72 h (B). The replication level of HCV RNA was monitored by the RL assay. The relative RL activity is shown. The results shown are means from three independent experiments; error bars indicate standard deviations. The results of Western blot analysis of cellular lysates with anti-HCV core or anti-β-actin antibody in OR6 cells at 72 h after the treatment with 1 μM ATO alone and in combination with 100 μM VC, with or without 10 mM NAC, are also shown. (C) Effect of combination treatment with ATO and the iNOS inhibitor 1400W on HCV RNA replication. OR6 cells were treated with 1 μM ATO alone and in combination with 1400W at the indicated concentrations for 72 h. The replication level of HCV RNA was monitored by the RL assay as described for panels A and B. (D and E) Effect of ATO on production of a ROS, O_2^-, in O cells. O cells were treated with 1 μM ATO (D) or 2 μM BSO (E) for 24 h. The intracellular O_2^- level was measured by flow cytometry using DHE as described in Materials and Methods. (F) Inhibition of ATO-dependent O_2^- induction by NAC. O cells were treated with either 1 μM ATO or 10 mM NAC alone and in combination with 10 mM NAC for 24 h. (G and H) Effect of ATO on production of a ROS, H_2O_2, in O cells. O cells were treated with 1 μM ATO (G) or 2 μM BSO (H) for 24 h. The intracellular H_2O_2 level was measured by flow cytometry using DCF as described in Materials and Methods. (I) Effect of ATO on the intracellular glutathione level in O cells. O cells were treated with 1 μM ATO for 72 h. The intracellular glutathione level was measured by flow cytometry using CellTracker Green CMFDA as described in Materials and Methods.

tively activate STAT3 and NF-κB, which are associated with HCV pathogenesis (19, 34, 36, 43, 49, 59, 60, 67). In fact, oxidative stress has been shown to trigger STAT3 tyrosine phosphorylation and nuclear translocation, which correlate with the activation of STAT3, leading to its DNA-binding activity (9). In contrast, ATO inhibited the STAT3 tyrosine phosphorylation through direct interaction with JAK kinase, thereby suppressing the transcriptional activity of STAT3 (12, 62). Importantly, STAT3 activation has been reported to be associated with HCV RNA replication (59, 69). The STAT3 Tyr705 dominant negative mutant has been shown to inhibit HCV RNA replication, suggesting that STAT3 positively regulates HCV replication (59). In contrast, others have reported that STAT3 induces anti-HCV activity (69). In this study, we analyzed the potential effect of ATO treatment on a set of stress-signaling events, including the NF-κB, AP-1, and STAT3 pathways, since ATO is known to modulate various signaling pathways. However, at 1 μM, which exerted an anti-HCV activity, the respective signaling pathways were not affected, arguing that the anti-HCV activity is independent of these

pathways (Fig. 5). In this regard, these stress-signaling pathways have been reported to be constitutively activated in HCV core- or NS5A-expressing cells (19, 36, 49, 59, 60, 67). In addition, previous studies demonstrated that ATO modulates the NF-κB, AP-1, and STAT3 pathways at higher concentrations (NF-κB, >10 μM; AP-1, >30 μM; STAT3, >4 μM). Therefore, we may have only observed the marginal effect of ATO in this study (Fig. 5). On the other hand, the HCV core or NS3 protein as well as HCV infection induces NO, leading to induction of double-stranded DNA breaks and accumulation of mutations of cellular genes (35). However, the iNOS inhibitor 1400W could not suppress HCV RNA replication and the anti-HCV activity of ATO, indicating that NO is not associated with the anti-HCV activity or with HCV replication (Fig. 6C).

It has been indicated that oxidative damage plays an important role in the effect of ATO (38). ROS generated in response to ATO exposure lead to accumulation of intracellular H_2O_2. Glutathione peroxidase and catalase are key enzymes regulating the levels of ROS and protecting cells from ATO-induced damage (26). However, the gastrointestinal glutathione peroxidase was drastically downregulated in cells harboring HCV replicons, which are rendered more susceptible to oxidative stress (39). The glutathione redox system has been implicated in the cellular defense system (14, 20). Glutathione, a major antioxidant in cells, is a tripeptide synthesized from cysteine, glutamic acid, and glycine, and it can scavenge superoxide anion free radicals. ATO has been shown to bind to the sulfhydryl group of glutathione and deplete the intracellular glutathione, resulting in enhancement of the sensitivity to oxidative damage (20, 33). Conversely, the antioxidant NAC is readily taken up by cells and serves as a precursor to elevate intracellular glutathione (53). In fact, ATO-induced apoptosis has been shown to be inhibited by NAC (11, 14, 21, 28). In this study, we have demonstrated that the anti-HCV activity of ATO was completely eliminated by treatment with NAC for 24 h (Fig. 6A). In addition, we found that ATO increased intracellular O_2^- but not H_2O_2 and depleted the intracellular glutathione in HCV RNA-replicating cells (Fig. 6D to I). Importantly, NAC diminished the ATO-dependent O_2^- induction (Fig. 6F). This finding could strengthen the link between ATO-dependent oxidative stress and anti-HCV activity. Similarly, Wen et al. reported an increase in ROS and enhanced susceptibility to glutathione depletion in the HCV core-expressing HepG2 cells (61). Accordingly, ROS have been shown to significantly suppress RNA replication in HCV replicon-harboring cells treated with H_2O_2 (13). In addition, HCV replication has been shown to be inhibited by lipid peroxidation of arachidonate, and this peroxidation could be blocked by lipid-soluble antioxidants such as vitamin E (23). Conversely, several antioxidants, such as vitamin C, vitamin E, and NAC, enhanced HCV replication in the present study (Fig. 6A and B) (65). Thus, we suggest that ATO inhibited HCV RNA replication by modulating the glutathione redox system and oxidative stress. In contrast to the above findings with HCV, NAC has been shown to suppress HIV-1 replication by preventing the activation of HIV-1 long terminal repeat transcription by NF-κB, suggesting a correlation between a decrease in glutathione levels and activation of HIV-1 replication (46, 53, 54). In this context, ATO has shown opposite effects on HIV-1 and HCV replication, stimulating the former and inhibiting the latter. Considering all of these results together, ATO can be regarded as a useful, novel anti-HCV reagent. In addition, the host redox system may be critical for HCV replication and may represent a pivotal target for the clinical treatment of patients with chronic hepatitis C.

ACKNOWLEDGMENTS

We thank D. Trono, R. Agami, R. Iggo, A. Takamizawa, T. Hirano, A. Yoshimura, and M. Hijikata for the VSV G-pseudotyped HIV-1-based vector system pCMVΔR8.91, pMDG2, pSUPER, pRDI292, anti-NS5A antibody, APRE-Luc, and 293FT cells. We also thank T. Stamminger, M. Yano, and T. Nakamura for their helpful suggestions and technical assistance.

This work was supported by a Grant-in-Aid for Scientific Research (C) from the Japan Society for the Promotion of Science (JSPS); by a Grant-in-Aid for Research on Hepatitis from the Ministry of Health, Labor, and Welfare of Japan; by the Kawasaki Foundation for Medical Science and Medical Welfare; by the Okayama Medical Foundation; and by the Ryobi Teien Memorial Foundation.

REFERENCES

1. **Ariumi, Y., T. Priscilla, M. Masutani, and D. Trono.** 2005. DNA damage sensors ATM, ATR, DNA-PKcs, and PARP-1 are dispensable for human immunodeficiency virus type 1 integration. J. Virol. **79:**2973–2978.
2. **Ariumi, Y., M. Kuroki, K. Abe, H. Dansako, M. Ikeda, T. Wakita, and N. Kato.** 2007. DDX3 DEAD-box RNA helicase is required for hepatitis C virus RNA replication. J. Virol. **81:**13922–13926.
3. **Ariumi, Y., M. Kuroki, H. Dansako, K. Abe, M. Ikeda, T. Wakita, and N. Kato.** 2008. The DNA damage sensors, ataxia-telangiectasia mutated kinase and checkpoint kinase 2 are required for hepatitis C virus RNA replication. J. Virol. **82:**9639–9646.
4. **Benali-Furet, N. L., M. Chami, L. Houel, F. De Giorgi, F. Vernejoul, D. Lagorce, L. Buscail, R. Bartenschlager, F. Ichas, R. Rizzuto, and P. Paterlini-Bréchot.** 2005. Hepatitis C virus core triggers apoptosis in liver cells by inducing ER stress and ER calcium depletion. Oncogene **24:**4921–4933.
5. **Berthoux, L., G. J. Towers, C. Gurer, P. Salomoni, P. P. Pandolfi, and J. Luban.** 2003. As2O3 enhances retroviral reverse transcription and counteracts Ref1 antiviral activity. J. Virol. **77:**3167–3180.
6. **Berthoux, L., S. Sebastian, E. Sokolskaja, and J. Luban.** 2004. Lv1 inhibition of human immunodeficiency virus type 1 is counteracted by factors that stimulate synthesis or nuclear translocation of viral cDNA. J. Virol. **78:**11739–11750.
7. **Bridge, A. J., S. Pebernard, A. Ducraux, A. L. Nicoulaz, and R. Iggo.** 2003. Induction of an interferon response by RNAi vectors in mammalian cells. Nat. Genet. **34:**263–264.
8. **Brummelkamp, T. R., R. Bernard, and R. Agami.** 2002. A system for stable expression of short interfering RNAs in mammalian cells. Science **296:**550–553.
9. **Carballo, M., M. Conde, R. E. Bekay, J. Martín-Nieto, M. J. Camacho, J. Monteseirín, J. Conde, F. J. Bedoya, and F. Sobrino.** 1999. Oxidative stress triggers STAT3 tyrosine phosphorylation and nuclear translocation in human lymphocytes. J. Biol. Chem. **274:**17580–17586.
10. **Cavigelli, M., W. W. Li, A. Lin, B. Su, K. Yoshioka, and M. Karin.** 1996. The tumor promoter arsenite stimulates AP-1 activity by inhibiting a JNK phosphatase. EMBO J. **15:**6269–6279.
11. **Chen, Y. C., S. Y. Lin-Shiau, and J. K. Lin.** 1998. Involvement of reactive oxygen species and caspase 3 activation in arsenite-induced apoptosis. J. Cell Physiol. **177:**324–333.
12. **Cheng, H. Y., P. Li, M. David, T. E. Smithgall, L. Feng, and M. W. Lieberman.** 2004. Arsenic inhibition of the JAK-STAT pathway. Oncogene **23:**3603–3612.
13. **Choi, J., K. J. Lee, Y. Zheng, A. K. Yamaga, M. M. C. Lai, and J. H. Ou.** 2004. Reactive oxygen species suppress hepatitis C virus RNA replication in human hepatoma cells. Hepatology **39:**81–89.
14. **Dai, J., R. S. Weinberg, S. Waxman, and Y. Jing.** 1999. Malignant cells can be sensitized to undergo growth inhibition and apoptosis by arsenic trioxide through modulation of the glutathione redox system. Blood **93:**268–277.
15. **Davis, G. L.** 2006. Tailoring antiviral therapy in hepatitis C. Hepatology **43:**909–911.
16. **De Maria, N., A. Colantoni, S. Fagiuoli, G. J. Liu, B. K. Rogers, F. Farinati, D. H. Van Thiel, and R. A. Floyd.** 1996. Association between reactive oxygen species and disease activity in chronic hepatitis C. Free Radic. Biol. Med. **21:**291–295.
17. **Everett, R. D., and M. K. Chelbi-Alix.** 2007. PML and PML nuclear bodies: implications in antiviral defence. Biochemie **89:**819–830.
18. **Farinati, F., R. Cardin, N. De Maria, G. D. Libera, C. Marafin, E. Lecis, P.**

Burra, A. Floreani, A. Cecchetto, and R. Naccarato. 1995. Iron storage, lipid peroxidation and glutathione turnover in chronic anti-HCV positive hepatitis. J. Hepatol. **22:**449–456.
19. **Gong, G., G. Waris, R. Tanveer, and A. Siddiqui.** 2001. Human hepatitis C virus NS5A protein alters intracellular calcium levels, induces oxidative stress, and activates STAT-3 and NF-κB. Proc. Natl. Acad. Sci. USA **98:** 9599–9604.
20. **Han, Y. H., S. H. Kim, S. Z. Kim, and W. H. Park.** 2008. Apoptosis in arsenic trioxide-treated Calu-6 lung cells is correlated with the depletion of GSH levels rather than the change of ROS levels. J. Cell. Biochem. **104:**862–878.
21. **Han, Y. H., S. Z. Kim, S. H. Kim, and W. H. Park.** 2008. Suppression of arsenic trioxide-induced apoptosis in HeLa cells by N-acetylcysteine. Molecules Cells **26:**18–25.
22. **Herzer, K., S. Weyer, P. H. Krammer, P. R. Galle, and T. G. Hofmann.** 2005. Hepatitis C virus core protein inhibits tumor suppressor protein promyelocytic leukemia function in human hepatoma cells. Cancer Res. **65:**10830–10837.
23. **Huang, H., Y. Chen, and J. Ye.** 2007. Inhibition of hepatitis C virus replication by peroxidation of arachidonate and restoration by vitamin E. Proc. Natl. Acad. Sci. USA **104:**18666–18670.
24. **Hwang, D. R., Y. C. Tsai, J. C. Lee, K. K. Huang, R. K. Lin, C. H. Ho, J. M. Chiou, Y. T. Lin, J. T. A. Hsu, and C. T. Yeh.** 2004. Inhibition of hepatitis C virus replication by arsenic trioxide. Antimicrob. Agents Chemother. **48:** 2876–2882.
25. **Ikeda, M., K. Abe, H. Dansako, T. Nakamura, K. Naka, and N. Kato.** 2005. Efficient replication of a full-length hepatitis C virus genome, strain O, in cell culture, and development of a luciferase reporter system. Biochem. Biophys. Res. Commun. **329:**1350–1359.
26. **Jing, Y., J. Dai, R. M. E. Chalmers-Redman, W. G. Tatton, and S. Waxman.** 1999. Arsenic trioxide selectively induces acute promyelocytic leukemia cell apoptosis via a hydrogen peroxide-depndent pathway. Blood **94:**2102–2111.
27. **Joe, Y., J. H. Jeong, S. Yang, H. Kang, N. Motoyama, P. P. Pandolfi, J. H. Chung, and M. K. Kim.** 2006. ATR, PML, and Chk2 play a role in arsenic trioxide-induced apoptosis. J. Biol. Chem. **281:**28764–28771.
28. **Kang, Y. H., M. J. Yi, M. J. Kim, M. T. Park, S. Bae, C. M. Kang, C. K. Cho, I. C. Park, M. J. Park, C. H. Rhee, S. I. Hong, H. Y. Chung, Y. S. Lee, and S. J. Lee.** 2004. Caspase-independent cell death by arsenic trioxide in human cervical cancer cells: reactive oxygen species-mediated poly(ADP-ribose) polymerase-1 activation signals apoptosis-inducing factor release from mitochondria. Cancer Res. **64:**8960–8967.
29. **Kapahi, P., T. Takahashi, G. Natoli, S. R. Adams, Y. Chen, R. Y. Tsien, and M. Karin.** 2000. Inhibition of NF-κB activation by arsenite through reaction with a critical cysteine in the activation loop of IκB kinase. J. Biol. Chem. **275:**36062–36066.
30. **Kato, N.** 2001. Molecular virology of hepatitis C virus. Acta Med. Okayama **55:**133–159.
31. **Kato, N., K. Sugiyama, K. Namba, H. Dansako, T. Nakamura, M. Takami, K. Naka, A. Nozaki, and K. Shimotohno.** 2003. Establishment of a hepatitis C virus subgenomic replicon derived from human hepatocytes infected in vitro. Biochem. Biophys. Res. Commun. **306:**756–766.
32. **Keckesova, Z., L. M. J. Ylinen, and G. J. Towers.** 2004. The human and African green monkey TRIM5α genes encode Ref1 and Lv1 retroviral restriction factor activities. Proc. Natl. Acad. Sci. USA **101:**10780–10785.
33. **Kito, M., Y. Akao, N. Ohishi, K. Yagi, and Y. Nozawa.** 2002. Arsenic trioxide-induced apoptosis and its enhancement by buthionine sulfoximine in hepatocellular carcinoma cell lines. Biochem. Biophys. Res. Commun. **291:**861–867.
34. **Korenaga, M., T. Wang, Y. Li, L. A. Showalter, T. Chan, J. Sun, and S. A. Weinman.** 2005. Hepatitis C virus core protein inhibits mitochondrial electron transport and increases reactive oxygen species (ROS) production. J. Biol. Chem. **280:**37481–37488.
35. **Machida, K., K. T. Cheng, V. M. Sung, K. J. Lee, A. M. Levine, and M. M. C. Lai.** 2004. Hepatitis C virus infection activates the immunologic (type II) isoform of nitric oxide synthase and thereby enhances DNA damage and mutations of cellular genes. J. Virol. **78:**8835–8843.
36. **Machida, K., K. T. H. Cheng, C. K. Lai, K. S. Jeng, V. M. H. Sung, and M. M. C. Lai.** 2006. Hepatitis C virus triggers mitochondrial permeability transition with production of reactive oxygen species, leading to DNA damage and STAT3 activation. J. Virol. **80:**7199–7207.
37. **Meyer, M., R. Schreck, and P. A. Baeuerle.** 1993. H_2O_2 and antioxidants have opposite effects on activation of NF-κB and AP-1 in intact cells: AP-1 as secondary antioxidant-responsive factor. EMBO J. **12:**2005–2015.
38. **Miller, W. H., Jr., H. M. Schipper, J. S. Lee, J. Singer, and S. Waxman.** 2002. Mechanisms of action of arsenic trioxide. Cancer Res. **62:**3893–3903.
39. **Morbitzer, M., and T. Herget.** 2005. Expression of gastrointestinal glutathione peroxidase is inversely correlated to the presence of hepatitis C virus subgenomic RNA in human liver cells. J. Biol. Chem. **280:**8831–8841.
40. **Moriya, K., K. Nakagawa, T. Santa, Y. Shintani, H. Fujie, H. Miyoshi, T. Tsutsumi, T. Miyazawa, K. Ishibashi, T. Horie, K. Imai, T. Todoroki, S. Kimura, and K. Koike.** 2001. Oxidative stress in the absence of inflammation in a mouse model for hepatitis C virus-associated hepatocarcinogenesis. Cancer Res. **61:**4365–4370.
41. **Nakajima, K., Y. Yamanaka, K. Nakae, H. Kojima, M. Ichiba, N. Kiuchi, T. Kitaoka, T. Fukada, M. Hibi, and T. Hirano.** 1996. A central role for STAT3 in IL-6-induced regulation of growth and differentiation in M1 leukemia cells. EMBO J. **15:**3651–3658.
42. **Naldini, L., U. Blömer, P. Gallay, D. Ory, R. Mulligan, F. H. Gage, I. M. Verma, and D. Trono.** 1996. In vivo gene delivery and stable transduction of nondividing cells by a lentiviral vector. Science **272:**263–267.
43. **Okuda, M., K. Li, M. R. Beard, L. A. Showalter, F. Scholle, S. M. Lemon, and S. A. Weinman.** 2002. Mitochondrial injury, oxidative stress, and antioxidant gene expression are induced by hepatitis C virus core protein. Gastroenterology **122:**366–375.
44. **Pion, M., R. Stalder, R. Correa, B. Mangeat, G. J. Towers, and V. Piguet.** 2007. Identification of an arsenic-sensitive block to primate lentiviral infection of human dendritic cells. J. Virol. **81:**12086–12090.
45. **Porter, A. C., G. R. Fanger, and R. R. Vaillancourt.** 1999. Signal transduction pathways regulated by arsenate and arsenite. Oncogene **18:**7794–7802.
46. **Roederer, M., F. J. T. Staal, P. A. Raju, S. W. Ela, L. A. Herzenberg, and L. A. Herzenberg.** 1990. Cytokine-stimulated human immunodeficiency virus replication is inhibited by *N*-acetyl-L-cysteine. Proc. Natl. Acad. Sci. USA **87:**4884–4888.
47. **Saenz, D. T., W. Teo, J. C. Olsen, and E. M. Poeschla.** 2005. Restriction of feline immunodeficiency virus by Ref1, Lv1, and primate TRIM5α proteins. J. Virol. **79:**15175–15188.
48. **Sakurai, T., T. Kaise, and C. Matsubara.** 1998. Inorganic and methylated arsenic compounds induce cell death in murine macrophages via different mechanisms. Chem. Res. Toxicol. **11:**273–283.
49. **Sarcar, B., A. K. Ghosh, R. Steele, R. Ray, and R. B. Ray.** 2004. Hepatitis C virus NS5A mediated STAT3 activation requires co-operation of Jak1 kinase. Virology **322:**51–60.
50. **Sayah, D. M., and J. Luban.** 2004. Selection for loss of Ref1 activity in human cells releases human immunodeficiency virus type 1 from cyclophilin A dependence during infection. J. Virol. **78:**12066–12070.
51. **Shen, Z. X., G. Q. Chen, J. H. Ni, X. S. Li, S. M. Xiong, Q. Y. Qiu, J. Zhu, W. Tang, G. L. Sun, K. Q. Yang, Y. Chen, L. Zhou, Z. W. Fang, Y. T. Wang, J. Ma, P. Zhang, T. D. Zhang, S. J. Chen, Z. Chen, and Z. Y. Wang.** 1997. Use of arsenic trioxide (As_2O_3) in the treatment of acute promyelocytic leukemia (APL). II. Clinical efficacy and pharmacokinetics in relapsed patients. Blood **89:**3354–3360.
52. **Soignet, S. L., P. Maslak, Z. G. Wang, S. Jhanwar, E. Calleja, L. J. Dardashti, D. Corso, A. DeBlasio, J. Gabrilove, D. A. Scheinberg, P. P. Pandolfi, and R. P. Warrell, Jr.** 1998. Complete remission after treatment of acute promyelocytic leukemia with arsenic trioxide. N. Engl. J. Med. **339:**1341–1348.
53. **Staal, F. J. T., M. Roederer, L. A. Herzenberg, and L. A. Herzenberg.** 1990. Intracellular thiols regulate activation of nuclear factor κB and transcription of human immunodeficiency virus. Proc. Natl. Acad. Sci. USA **87:**9943–9947.
54. **Staal, F. J. T., S. W. Ela, M. Roederer, M. T. Anderson, L. A. Herzenberg, and L. A. Herzenberg.** 1992. Glutathione deficiency and human immunodeficiency virus infection. Lancet **339:**909–912.
55. **Tardif, K. D., K. Mori, and A. Siddiqui.** 2002. Hepatitis C virus subgenomic replicons induce endoplasmic reticulum stress activating an intracellular signaling pathway. J. Virol. **76:**7453–7459.
56. **Tavalai, N., P. Papior, S. Rechter, M. Leis, and T. Stamminger.** 2006. Evidence for a role of the cellular ND10 protein PML in mediating intrinsic immunity against human cytomegalovirus infections. J. Virol. **80:**8006–8018.
57. **Turelli, P., V. Doucas, E. Craig, B. Mangeat, N. Klages, R. Evans, G. Kalpana, and D. Trono.** 2001. Cytoplasmic recruitment of INI1 and PML on incoming HIV preintegration complexes: interference with early steps of viral replication. Mol. Cell **7:**1245–1254.
58. **Wakita, T., T. Pietschmann, T. Kato, T. Date, M. Miyamoto, Z. Zhao, K. Murthy, A. Habermann, H. G. Kräusslich, M. Mizokami, R. Bartenschlager, and T. J. Liang.** 2005. Production of infectious hepatitis C virus in tissue culture from a cloned viral genome. Nat. Med. **11:**791–796.
59. **Waris, G., J. Turson, T. Hassanein, and A. Siddiqui.** 2005. Hepatitis C virus (HCV) constitutively activates STAT-3 via oxidative stress: role of STAT3 in HCV replication. J. Virol. **79:**1569–1580.
60. **Waris, G., A. Livolsi, V. Imbert, J. F. Peyron, and A. Siddiqui.** 2003. Hepatitis C virus NS5A and subgenomic replicon activate NF-κB via tyrosine phosphorylation of IkBa and its degradation by calpain protease. J. Biol. Chem. **278:**40778–40787.
61. **Wen, F., M. Y. Abdalla, C. Aloman, J. Xiang, I. M. Ahmad, J. Walewski, M. L. McCormick, K. E. Brown, A. D. Branch, D. R. Spitz, B. E. Britigan, and W. N. Schmidt.** 2004. Increased prooxidant production and enhanced susceptibility to glutathione depletion in HepG2 cells co-expressing HCV core protein and CYP2E1. J. Med. Virol. **72:**230–240.
62. **Wetzler, M., M. T. Brady, E. Tracy, Z. R. Li, K. A. Donohue, K. L. O'Loughlin, Y. Cheng, A. Mortazavi, A. A. McDonald, P. Kunapuli, P. K. Wallace, M. R. Baer, J. K. Cowell, and H. Baumann.** 2006. Arsenic trioxide affects signal transducer and activator of transcription proteins through alteration of protein tyrosine kinase phosphorylation. Clin. Cancer Res. **12:** 6817–6825.

63. **Yang, S., C. Kuo, J. E. Bisi, and M. K. Kim.** 2002. PML-dependent apoptosis after DNA damage is regulated by the checkpoint kinase hCds1/Chk2. Nat. Cell Biol. **4:**865–870.
64. **Yang, S., J. H. Jeong, A. L. Brown, C. H. Lee, P. P. Pandolfi, J. H. Chung, and M. K. Kim.** 2006. Promyelocytic leukemia activates Chk2 by mediating Chk2 autophosphorylation. J. Biol. Chem. **281:**26645–26654.
65. **Yano, M., M. Ikeda, K. Abe, H. Dansako, S. Ohkoshi, Y. Aoyagi, and N. Kato.** 2007. Comprehensive analysis of the effects of ordinary nutrients on hepatitis C virus RNA replication in cell culture. Antimicrob. Agents Chemother. **51:**2016–2027.
66. **Yoda, A., K. Toyoshima, Y. Watanabe, N. Onishi, Y. Hazaka, Y. Tsukuda, J. Tsukada, T. Kondo, Y. Tanaka, and Y. Minami.** 2008. Arsenic trioxide augments Chk2/p53-mediated apoptosis by inhibiting oncogenic Wip1 phosphatase. J. Biol. Chem. **283:**18969–18979.
67. **Yoshida, T., T. Hanada, T. Tokuhisa, K. Kosai, M. Sata, M. Kohara, and A. Yoshimura.** 2002. Activation of STAT3 by the hepatitis C virus core protein leads to cellular transformation. J. Exp. Med. **196:**641–653.
68. **Zhang, P., S. Y. Wang, and X. H. Hu.** 1996. Arsenic trioxide treated 72 cases of acute promyelocytic leukemia. Chin. J. Hematol. **17:**58–62.
69. **Zhu, H., X. Shang, N. Terada, and C. Liu.** 2004. STAT3 induces anti-hepatitis C viral activity in liver cells. Biochem. Biophys. Res. Commun. **324:**518–528.
70. **Zhu, J., M. H. M. Koken, F. Quignon, M. K. Chelbi-Alix, L. Degos, Z. Y. Wang, Z. Chen, and H. de Thé.** 1997. Arsenic-induced PML targeting onto nuclear bodies: implications for the treatment of acute promyelocytic leukemia. Proc. Natl. Acad. Sci. USA **94:**3978–3983.
71. **Zufferey, R., D. Nagy, R. J. Mandel, L. Naldini, and D. Trono.** 1997. Multiply attenuated lentiviral vector achieves efficient gene delivery in vivo. Nat. Biotechnol. **15:**871–875.

JOURNAL OF VIROLOGY, Oct. 2008, p. 9639–9646 Vol. 82, No. 19
0022-538X/08/$08.00+0 doi:10.1128/JVI.00351-08

The DNA Damage Sensors Ataxia-Telangiectasia Mutated Kinase and Checkpoint Kinase 2 Are Required for Hepatitis C Virus RNA Replication▽

Yasuo Ariumi,[1] Misao Kuroki,[1] Hiromichi Dansako,[1] Ken-Ichi Abe,[1] Masanori Ikeda,[1] Takaji Wakita,[2] and Nobuyuki Kato[1]*

Department of Molecular Biology, Okayama University Graduate School of Medicine, Dentistry, and Pharmaceutical Sciences, 2-5-1, Shikata-cho, Okayama 700-8558, Japan,[1] and Department of Virology II, National Institute of Infectious Diseases, 1-23-1 Toyama, Shinjuku-ku, Tokyo 162-8640, Japan[2]

Received 18 February 2008/Accepted 18 July 2008

Cellular responses to DNA damage are crucial for maintaining genome integrity, virus infection, and preventing the development of cancer. Hepatitis C virus (HCV) infection and the expression of the HCV nonstructural protein NS3 and core protein have been proposed as factors involved in the induction of double-stranded DNA breaks and enhancement of the mutation frequency of cellular genes. Since DNA damage sensors, such as the ataxia-telangiectasia mutated kinase (ATM), ATM- and Rad3-related kinase (ATR), poly(ADP-ribose) polymerase 1 (PARP-1), and checkpoint kinase 2 (Chk2), play central roles in the response to genotoxic stress, we hypothesized that these sensors might affect HCV replication. To test this hypothesis, we examined the level of HCV RNA in HuH-7-derived cells stably expressing short hairpin RNA targeted to ATM, ATR, PARP-1, or Chk2. Consequently, we found that replication of both genome-length HCV RNA (HCV-O, genotype 1b) and the subgenomic replicon RNA were notably suppressed in ATM- or Chk2-knockdown cells. In addition, the RNA replication of HCV-JFH1 (genotype 2a) and the release of core protein into the culture supernatants were suppressed in these knockdown cells after inoculation of the cell culture-generated HCV. Consistent with these observations, ATM kinase inhibitor could suppress the HCV RNA replication. Furthermore, we observed that HCV NS3-NS4A interacted with ATM and that HCV NS5B interacted with both ATM and Chk2. Taken together, these results suggest that the ATM signaling pathway is critical for HCV RNA replication and may represent a novel target for the clinical treatment of patients with chronic hepatitis C.

Hepatitis C virus (HCV) infection frequently causes chronic hepatitis, which progresses to liver cirrhosis and hepatocellular carcinoma. HCV infection has now become a serious health problem, with at least 170 million people currently infected worldwide (28). HCV is an enveloped virus with a positive single-stranded 9.6-kb RNA genome, which encodes a large polyprotein precursor of approximately 3,000 amino acid residues. This polyprotein is cleaved by a combination of the host and viral proteases into at least 10 proteins in the following order: core, envelope 1 (E1), E2, p7, nonstructural 2 (NS2), NS3, NS4A, NS4B, NS5A, and NS5B (12, 13, 27).

Studies have shown that various viruses with distinct replication strategies—including the DNA viruses Epstein-Barr virus, herpes simplex virus 1, adenovirus, and simian virus 40 and the retrovirus human immunodeficiency virus type 1 (HIV-1)—can activate DNA damage response pathways and utilize these damage responses to facilitate their own viral reproduction and promote the survival of infected cells (2, 16, 17). In the case of HCV, it has been proposed that HCV infection causes double-stranded DNA (dsDNA) breaks and enhances the mutation frequency of cellular genes and that these effects are mediated by nitric oxide (18, 19). In addition, the HCV core, E1, and NS3 proteins have been suggested to be potent reactive oxygen species inducers, leading to DNA damage (19). Furthermore, we previously demonstrated that HCV NS5B-expressing PH5CH8 immortalized human hepatocyte cells were susceptible to DNA damage in the form of dsDNA breaks (23). Thus, HCV seems to be associated with the dsDNA damage response pathways.

Since the DNA damage sensors, such as ataxia-telangiectasia mutated kinase (ATM), ATM- and Rad3-related kinase (ATR), poly(ADP-ribose) polymerase 1 (PARP-1), and checkpoint kinase 2 (Chk2; a direct downstream target of ATM), play central roles in response to genotoxic stress (10), we hypothesized that these sensors might affect HCV replication.

To investigate the possible involvement of these cellular factors in HCV replication, we examined the level of HCV RNA in cells rendered defective for DNA damage sensors by RNA interference or by pharmacological inhibition.

MATERIALS AND METHODS

Cell culture. 293FT cells were cultured in Dulbecco's modified Eagle's medium (DMEM; Invitrogen, Carlsbad, CA) supplemented with 10% fetal bovine serum (FBS). The HuH-7-derived O cells harboring a replicative genome-length HCV RNA and the HuH-7-derived sO cells harboring the subgenomic replicon RNA of HCV-O were cultured in DMEM with 10% FBS and G418 (300 μg/ml geneticin; Invitrogen) as described previously (11, 14). Oc and sOc cells, which were created by eliminating HCV RNA from O cells and sO cells by interferon (IFN) treatment (11, 14), respectively, were also cultured in DMEM with 10% FBS.

RNA interference. Oligonucleotides with the following sense and antisense sequences were used for the cloning of short hairpin RNA (shRNA)-encoding se-

* Corresponding author. Mailing address: Department of Molecular Biology, Okayama University Graduate School of Medicine, Dentistry, and Pharmaceutical Sciences, 2-5-1, Shikata-cho, Okayama 700-8558, Japan. Phone: 81 86 235 7385. Fax: 81 86 235 7392. E-mail: nkato@md.okayama-u.ac.jp.

▽ Published ahead of print on 30 July 2008.

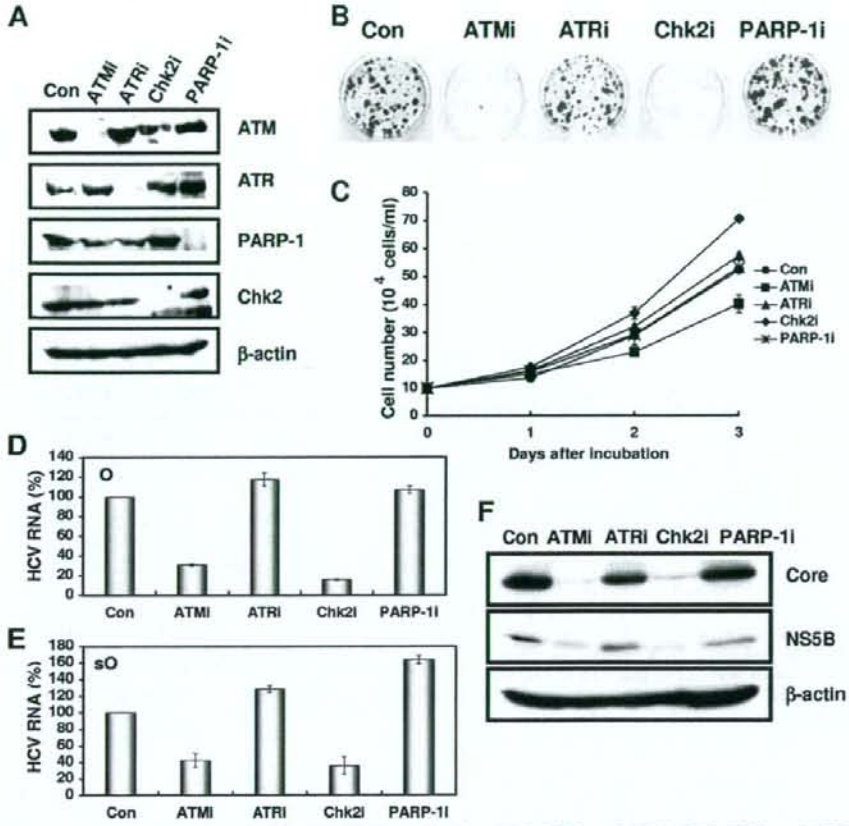

FIG. 1. The ATM signaling pathway is required for HCV RNA replication. (A) Inhibition of ATM, ATR, Chk2, or PARP-1 expression by shRNA-producing lentiviral vectors. The results of the Western blot analysis of cellular lysates with anti-ATM, anti-ATR, anti-Chk2, anti-PARP-1, or anti-β-actin antibody in Oc cells expressing shRNA targeted to ATM (ATMi), ATR (ATRi), Chk2 (Chk2i), or PARP-1 (PARP-1i) as well as in Oc cells transduced with a control lentiviral vector (Con) are shown. (B) ECF in ATM-, ATR-, Chk2-, or PARP-1-knockdown cells. In vitro transcribed ON/C-5B K1609E RNA (2 μg) was transfected into the ATM-, ATR-, Chk2, or PARP-1-knockdown Oc cells or the Oc cells transduced with a control lentiviral vector (Con). G418-resistant colonies were stained with Coomassie brilliant blue at 3 weeks after electroporation of RNA. Experiments were done in duplicate, and a representative result is shown. (C) The cell growth curve of ATM (ATMi), ATR (ATRi), Chk2 (Chk2i), or PARP-1 (PARP-1i)-knockdown Oc cells or the Oc cells transduced with a control lentiviral vector (Con). Results from three independent experiments are shown. (D) The level of genome-length HCV-O RNA was monitored by real-time LightCycler PCR (Roche). Experiments were done in triplicate, and columns represent the mean percentage of HCV RNA. (E) The level of subgenomic replicon (sO cells) RNA was monitored by real-time LightCycler PCR. Results from three independent experiments are shown as described in panel D. (F) The HCV core or NS5B protein expression level in ATM-, ATR-, Chk2-, or PARP-1-knockdown cells. The results of Western blot analysis of cellular lysates with anti-HCV core protein, anti-HCV NS5B, or anti-β-actin antibody in O cells expressing shRNA targeted to ATM (ATMi), ATR (ATRi), Chk2 (Chk2i), or PARP-1 (PARP-1i) as well as in O cells transduced with a control lentiviral vector (Con) are shown.

quences targeted to Chk2 in lentiviral vector: 5′-GATCCCCGGGGGAGAGCTGTT TGACATTCAAGAGATGTCAAACAGCTCTCCCCCTTTTTGGAAA-3′ (sense) and 5′-AGCTTTTCCAAAAAGGGGGAGAGCTGTTTGACATCTCTTGAATGT CAAACAGCTCTCCCCCGGG-3′ (antisense). The oligonucleotides above were annealed and subcloned into the BglII-HindIII site, downstream from an RNA polymerase III promoter of pSUPER (5), generating pSUPER-Chk2i. To construct pLV-Chk2i, the BamHI-SalI fragments of the pSUPER-Chk2i were subcloned into the BamHI-SalI site of pRDI292, an HIV-1-derived self-inactivating lentiviral vector containing a puromycin resistance marker allowing for the selection of transduced cells (4). pLV-ATMi, pLV-ATRi, and pLV-PARP-1i were constructed as described previously (1).

Lentiviral vector production. The vesicular stomatitis virus G protein (VSV-G)-pseudotyped HIV-1-based vector system has been described previously (24). The lentiviral vector particles were produced by transient transfection of the second-generation packaging construct pCMV-ΔR8.91 (30) and the VSV-G envelope plasmid pMDG2 as well as the lentiviral vector into 293FT cells with FuGene6 (Roche Diagnostics, Mannheim, Germany).

Quantitative reverse transcription-PCR analysis. Quantitative reverse transcription-PCR analysis for HCV RNA was performed by real-time LightCycler PCR as described previously (11).

Western blot analysis. Cells were lysed in buffer containing 50 mM Tris-HCl (pH 8.0), 150 mM NaCl, 4 mM EDTA, 1% Nonidet P-40, 0.1% sodium dodecyl sulfate (SDS), 1 mM dithiothreitol, and 1 mM phenylmethylsulfonyl fluoride. Supernatants from these lysates were subjected to SDS-polyacrylamide gel electrophoresis, followed by immunoblotting analysis using anti-ATM (2C1; GTX70103 [GeneTex, San Antonio, TX]), anti-ATR (GTX70133; GeneTex), anti-Chk2 (NT; ProSci, Poway, CA), anti-Chk2 (DCS-273; Medical and Biological Laboratories, Nagoya, Japan), anti-phospho-Chk2 (Thr68) (Cell Signaling,

Danvers, MA), anti-PARP-1 (C-2-10; Calbiochem, Merck Biosciences, Darmstadt, Germany), anti-hemagglutinin (HA) (HA-7; Sigma, St. Louis, MO), anti-core protein (CP-9 and CP-11; Institute of Immunology, Tokyo, Japan), anti-NS3 and anti-NS5B (no. 14; a generous gift from M. Kohara, the Tokyo Metropolitan Institute of Medical Science, Japan), anti-NS5A (no. 8926; a generous gift from A. Takamizawa, The Research Foundation for Microbial Diseases of Osaka University, Japan), and anti-β-actin (Sigma) Antibodies.

Immunofluorescence and confocal microscopic analysis. Cells were fixed in 3.5% formaldehyde in phosphate-buffered saline (PBS) and permeabilized in 0.1% NP-40 in PBS at room temperature. Cells were incubated with anti-ATM antibody (5C2; GTX70107 [GeneTex] or PM026 [MBL]), anti-HA antibody (3F10), anti-NS5B antibody and/or anti-NS3 antibody at a 1:300 dilution in PBS containing 3% bovine serum albumin at 37°C for 30 min. Cells were then stained with fluorescein isothiocyanate (FITC)-conjugated anti-rabbit antibody (Jackson ImmunoResearch, West Grove, PA) or anti-Cy3-conjugated anti-mouse antibody (Jackson ImmunoResearch) at a 1:300 dilution in PBS containing bovine serum albumin at 37°C for 30 min. Following extensive washing in PBS, cells were mounted on slides using a mounting medium of 90% glycerin–10% PBS with 0.01% *p*-phenylenediamine added to reduce fading. Samples were viewed under a confocal laser-scanning microscope (LSM510; Zeiss, Jena, Germany).

Immunoprecipitation. Cells were lysed in buffer containing 10 mM Tris-HCl (pH 8.0), 150 mM NaCl, 4 mM EDTA, 0.5% NP-40, 10 mM NaF, 1 mM dithiothreitol, and 1 mM phenylmethylsulfonyl fluoride. Lysates were precleared with 30 μl of protein G-Sepharose (GE Healthcare Biosciences, Uppsala, Sweden). Precleared supernatants were incubated with 5 μg of anti-HA antibody (3F10; Roche), 10 μl of anti-NS5B antibody, 5 μg of anti-Chk2 antibody (DCS-273; MBL), 5 μg of anti-FLAG antibody (M2; Sigma), or 5 μg of anti-ATM antibody (2C1) (GTX70103; GeneTex) at 4°C for 1 h. Following absorption of the precipitates on 30 μl of protein G-Sepharose resin for 1 h, the resin was washed four times with 700 μl of lysis buffer. Proteins were eluted by boiling the resin for 5 min in 2× Laemmli sample buffer. The proteins were then subjected to SDS-polyacrylamide gel electrophoresis, followed by immunoblotting analysis using anti-ATM, anti-Chk2, anti-HCV core protein (CP-9 and CP-11 mixture), anti-NS5A, anti-NS5B, anti-HA (HA-7; Sigma), or anti-NS3 antibody.

RESULTS

ATM and Chk2 are required for HCV RNA replication. To determine the potential role of DNA damage sensors in HCV replication, we first used lentiviral vector-mediated RNA interference to stably knockdown ATM, ATR, PARP-1 (1), or Chk2 in the following human hepatoma HuH-7-derived cell lines: O cells harboring a replicative genome-length HCV RNA (HCV-O, genotype 1b) (11), Oc cells derived from O cells (created by eliminating genome-length HCV RNA from O cells by IFN treatment) (11), sO cells harboring the subgenomic replicon of HCV-O (14), or RSc cells that cell culture-generated HCV (HCVcc) (JFH1, genotype 2a) (29) could infect and effectively replicate (3). To express shRNAs targeted to ATM, ATR, PARP-1 (1), or Chk2, we used a VSV-G-pseudotyped HIV-1-based vector system (24). We used puromycin-resistant pooled cells 10 days after the lentiviral transduction in all experiments. Western blot analysis of the lysates demonstrated very effective knockdown of ATM, ATR, Chk2, and PARP-1 in Oc cells (Fig. 1A). The effective knockdown of ATM, ATR, Chk2, or PARP-1 in O cells or sO cells was also confirmed by Western blot analysis (data not shown). In this context, the efficiency of colony formation (ECF) in ATM- or Chk2-, but not ATR- or PARP-1-, knockdown Oc cells transfected with the genome-length HCV-O RNA with an adapted mutation at amino acid position 1609 in the NS3 helicase region (ON/C-5B K1609E RNA) (11) was notably reduced compared with the control cells (Fig. 1B) even though Chk2-knockdown cells had a slightly faster growth rate than the control cells (Fig. 1C), suggesting that both ATM and Chk2 are crucial for HCV RNA replication. To further confirm this observation, we quantitatively examined the level of HCV RNA in the O cell- or sO cell-derived knockdown cells. Consequently, we found that replication of both genome-length HCV RNA (HCV-O) and its subgenomic replicon RNA (sO) were notably suppressed in ATM- or Chk2-knockdown cells but not in ATR- or PARP-1-knockdown cells (Fig. 1D and E). Consistent with this finding, the expression levels of core and NS5B proteins were also significantly decreased in the cell lysates of ATM- or Chk2-knockdown O cells (Fig. 1F). We next examined the replication level of HCV-JFH1 in ATM-, ATR-, Chk2-, or PARP-1-knockdown RSc cells (Fig. 2A). The results revealed that RNA replication of HCV-JFH1 and release of core protein into the culture supernatants were suppressed in only ATM- or Chk2-knockdown RSc cells after inoculation with HCVcc (Fig. 2B and C). Interestingly, the release of core protein into the culture supernatant was also significantly suppressed in ATR-knockdown RSc cells, while HCV RNA replication was slightly suppressed in these cells

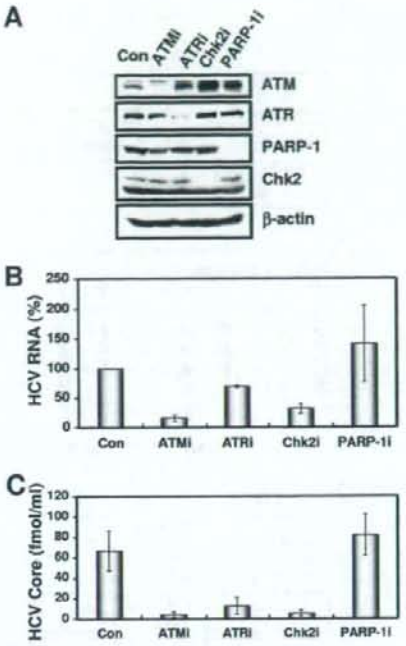

FIG. 2. ATM affects HCV infection. (A) Inhibition of ATM, ATR, Chk2, or PARP-1 expression by shRNA-producing lentiviral vectors. The results of Western blot analysis of cellular lysates with anti-ATM, anti-ATR, anti-PARP-1, anti-Chk2, or anti-β-actin antibody in RSc cured cells expressing shRNA targeted to ATM (ATMi), ATR (ATRi), Chk2 (Chk2i), or PARP-1 (PARP-1i) as well as in RSc cells transduced with a control lentiviral vector (Con) are shown. (B) The level of genome-length HCV (JFH1) RNA was monitored by real-time LightCycler PCR after inoculation of the HCVcc. Results from three independent experiments are shown as described in the legend of Fig. 1D. (C) The levels of the core protein in the culture supernatants were determined by enzyme-linked immunosorbent assay (Mitsubishi Kagaku Bio-Clinical Laboratories). Experiments were done in triplicate, and columns represent the mean core protein levels.

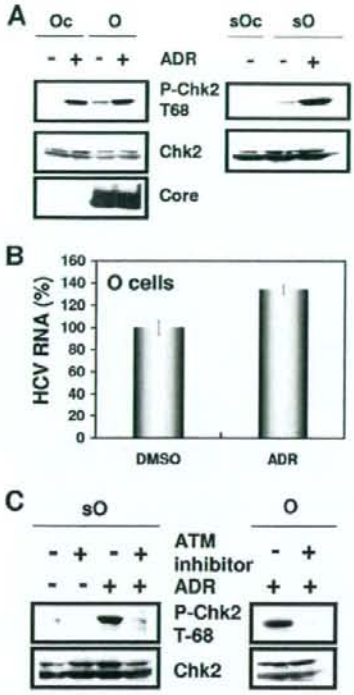

FIG. 3. ATM-dependent DNA damage response in HCV RNA-replicating cells. (A) Stimulation of Chk2 phosphorylation in the HCV RNA-replicating cells. The Oc, O, or sO cells were treated with 100 nM adriamycin (Sigma) for 2 h. The results of Western blot analysis of cellular lysates with anti-phospho-Chk2 (Thr68) (P-Chk2 T68), anti-Chk2, or anti-core protein antibody are shown. (B) Effect of adriamycin on HCV RNA replication. The O cells were treated with 100 nM adriamycin for 24 h. The level of genome-length HCV-O RNA was monitored by real-time LightCycler PCR. Results from three independent experiments are shown as described in the legend of Fig. 1D. DMSO, dimethyl sulfoxide. (C) Effect of ATM kinase inhibitor on Chk2 phosphorylation. The sO or O cells were pretreated with 10 μM ATM kinase inhibitor (KU-55933) (Calbiochem) for 2 h, followed by treatment with 100 nM adriamycin for 2 h. The results of Western blot analysis of cellular lysates with anti-phospho-Chk2 (Thr68) or anti-Chk2 antibody are shown.

(Fig. 2B and C), suggesting that ATR participates in the production of HCV virion.

In contrast, highly efficient knockdown of PARP-1 had no observable effects on the ECF (Fig. 1B), HCV RNA replication (Fig. 1D and E and 2B), or core protein expression in the cell lysate or in the supernatant (Fig. 1F and 2C), suggesting that our finding was not due to a nonspecific event. Thus, we have demonstrated for the first time that DNA damage sensors, ATM and Chk2, are required for HCV RNA replication.

ATM kinase activity in HCV RNA-replicating cells. Although it has been proposed that HCV causes dsDNA breaks (18, 19), little is known about whether HCV activates or inhibits the ATM-dependent damage response pathway. In this regard, it is worth noting that we observed weak but significant Chk2 phosphorylation at threonine 68, the specific marker for

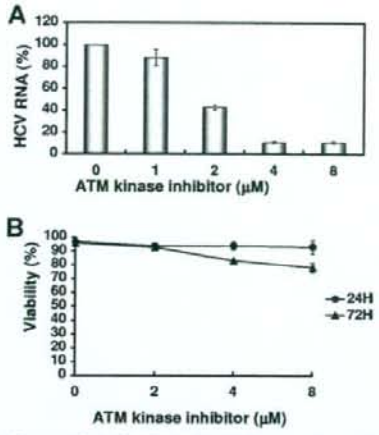

FIG. 4. Suppression of HCV RNA replication by ATM kinase inhibitor. (A) The level of genome-length HCV-O RNA was monitored by real-time LightCycler PCR after treatment with the indicated concentration of ATM kinase inhibitor for 72 h. Results from three independent experiments are shown as described in the legend of Fig. 1D. (B) Cell viabilities after treatment with the indicated concentration of ATM kinase inhibitor for 24 h or 72 h are shown.

ATM activation (20, 21), in the HCV RNA-replicating cells (O and sO cells) but not in the HCV-negative Oc and sOc cells (created by eliminating replicon RNA from sO cells by IFN treatment) (Fig. 3A), suggesting that the persistent HCV RNA replication stimulated the ATM-dependent DNA damage response. Furthermore, a 2-h treatment with 100 nM adriamycin, a dsDNA break inducer, markedly induced Chk2 phosphorylation in Oc, O, and sO cells (Fig. 3A). Importantly, Chk2 phosphorylation was not inhibited even in the HCV RNA-replicating cells (O and sO cells) (Fig. 3A), suggesting that the persistent HCV RNA replication and the HCV proteins are not able to suppress the ATM-dependent DNA damage response. To examine whether such a DNA damage response activates HCV RNA replication, we quantified the level of HCV RNA in the O cells treated with 100 nM adriamycin for 24 h. The results show that HCV RNA replication was increased (approximately 1.3-fold) after treatment with adriamycin (Fig. 3B), suggesting that the DNA damage response activates HCV RNA replication.

Suppression of HCV RNA replication by a small-molecule inhibitor of the ATM kinase. We next examined the effect of a specific small-molecule inhibitor of the ATM kinase (2-morpholin-4-yl-6-thianthren-1-yl-pyran-4-one [KU-55933]) (16) on HCV RNA replication. As expected, the ATM kinase inhibitor effectively inhibited Chk2 phosphorylation after adriamycin treatment in both sO and O cells (Fig. 3C). In this context, the ATM kinase inhibitor could efficiently suppress genome-length HCV RNA replication with an in vitro 50% effective concentration (EC_{50}) of approximately 2 μM at 72 h after treatment with adriamycin (Fig. 4A). Although this ATM kinase inhibitor did not affect cell viability at 24 h after the treatment, there was a slight decrease in the cell viability at 72 h after treatment (Fig. 4B). Thus, this or other ATM kinase inhibitors may be

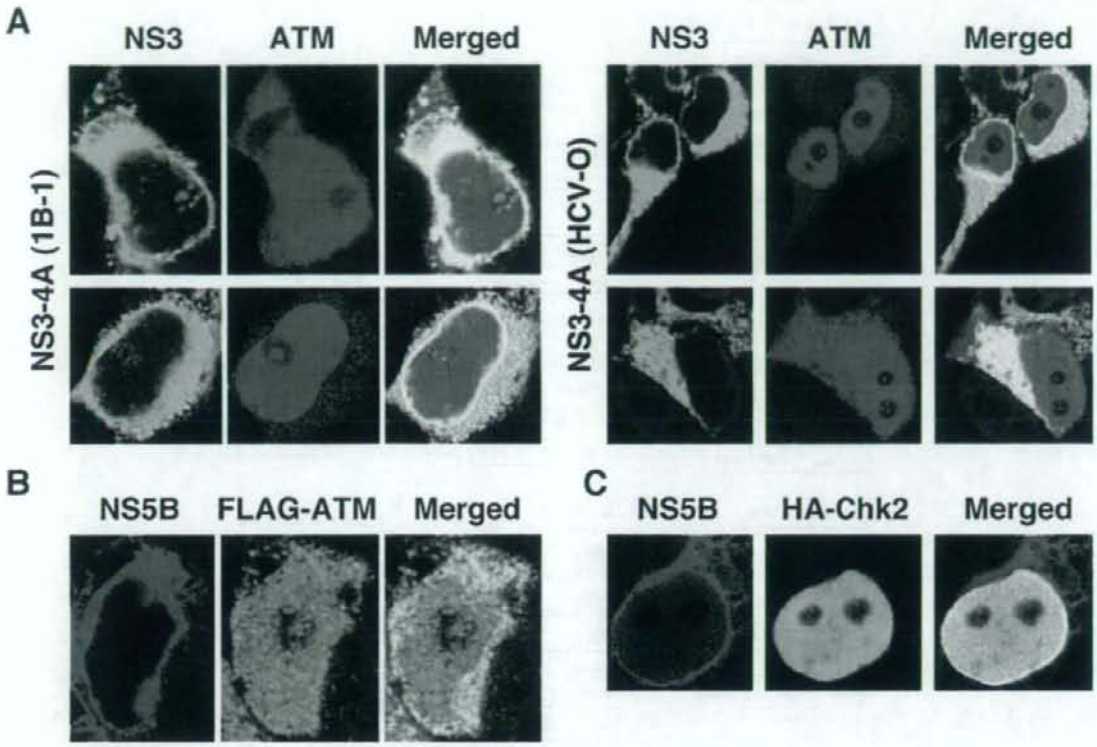

FIG. 5. Subcellular localization of ATM and Chk2 in HCV NS3-4A- or NS5B-expressing cells. (A) ATM partially colocalized with HCV NS3-4A. 293FT cells cotransfected with 300 ng of pCX4bsr/NS3-4A (1B-1) (8) or pCX4bsr/NS3-4A (O) (8) and 300 ng of pcDNA3-FLAG-ATMwt (6) were examined by confocal laser scanning microscopy. Cells were stained with anti-NS3 and anti-ATM (5C2) antibodies and then visualized with FITC (NS3) or Cy3 (ATM). (B) ATM partially colocalized with HCV NS5B. 293FT cells cotransfected with 300 ng of pCX4bsr/NS5B (1B-1) (23) and 300 ng of pcDNA3-FLAG-ATMwt (6). Cells were stained with anti-NS5B (no. 14) and anti-ATM (PM026) antibodies and then visualized with FITC (ATM) or Cy3 (NS5B). (C) Chk2 partially colocalized with HCV NS5B. 293FT cells cotransfected with 300 ng of pCX4bsr/NS5B (1B-1) (23) and 300 ng of pcDNA3-HA-Chk2wt (20, 21). Cells were stained with anti-NS5B and anti-HA (3F10) antibodies and then visualized with FITC (HA-Chk2) or Cy3 (NS5B). Images were visualized using confocal laser scanning microscopy (LSM510; Carl Zeiss). The right panels exhibit two-color overlay images (Merged). Colocalization is shown in yellow.

useful for the clinical treatment of patients with chronic hepatitis C.

Interaction of HCV NS3-4A with ATM. Since HCV NS3 has been proposed to be a viral factor involved in the induction of dsDNA breaks (18, 19), we first examined the subcellular localization of NS3-NS4A ([NS3-4A] 1B-1 or HCV-O strain) and ATM by confocal laser scanning microscopy. In most of the observed cells, ATM partially colocalized with NS3-4A in the perinuclear region and in dispersed points throughout the cytoplasm (Fig. 5A). In particular, we observed prominent colocalization of ATM with NS3-4A in some cells (Fig. 5A). Next, using anti-FLAG and anti-ATM antibodies, we immunoprecipitated lysates from 293FT cells in which FLAG-tagged ATM and either NS3-4A (HCV-O) or NS3 (HCV-O) were overexpressed and then performed immunoblotting analysis using either anti-ATM or anti-NS3 antibody to determine whether ATM binds to NS3-4A or NS3. The results revealed that ATM preferentially bound to NS3-4A over NS3 alone (Fig. 6A). Similarly, we found that ATM bound to NS3-4A using the O cell lysates (Fig. 6B), while HA-tagged Chk2 did not bind to NS3-4A in immunoprecipitation analysis using lysates from 293FT cells in which NS3-4A and HA-tagged Chk2 were overexpressed (Fig. 6C). Although NS3-4A has protease activity, ATM was not cleaved by the NS3-4A protease (Fig. 6D). Taking these results together, we conclude that ATM is able to interact with NS3-4A.

Interaction of HCV NS5B with ATM and Chk2. We next examined the subcellular localization of ATM and/or Chk2 in HCV NS5B-expressing cells by confocal laser scanning microscopy since we previously demonstrated that HCV NS5B-expressing PH5CH8 immortalized human hepatocyte cells were susceptible to DNA damage in the form of dsDNA breaks (23). ATM partially colocalized with NS5B in dispersed points throughout the cytoplasm (Fig. 5B), similar to the subcellular localization of HCV NS3-4A and ATM. Furthermore, Chk2 also partially colocalized with NS5B in the perinuclear region and in dispersed points in the nucleus (Fig. 5C). To determine whether endogenous ATM binds to NS5B, lysates from Oc or

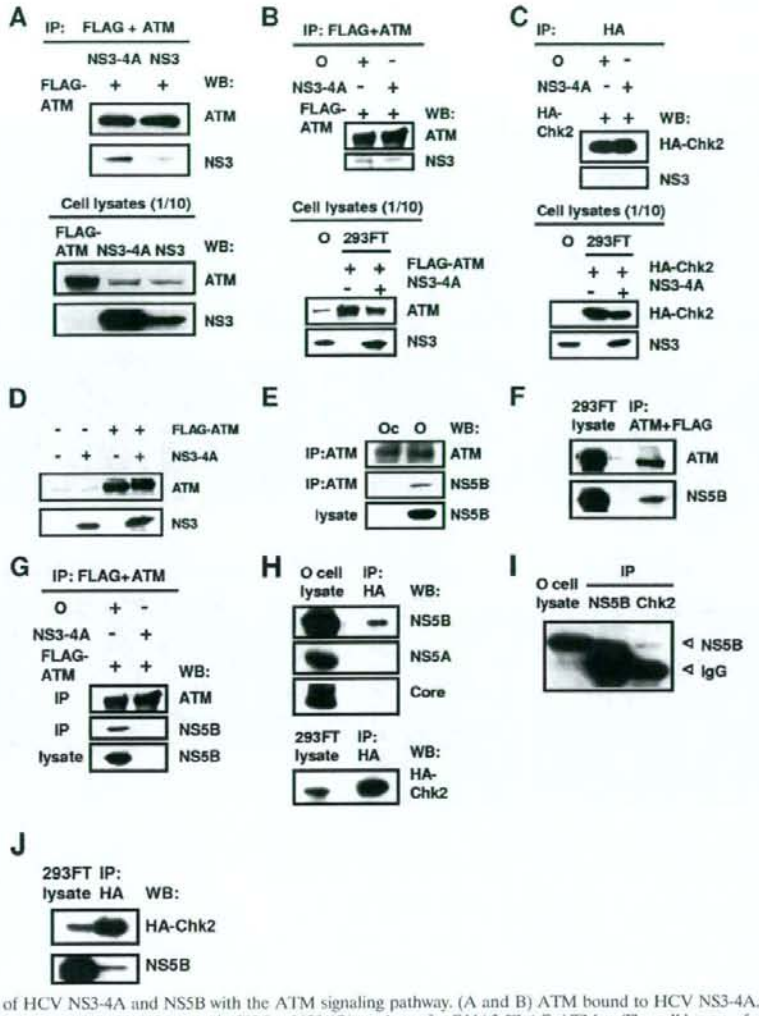

FIG. 6. Interaction of HCV NS3-4A and NS5B with the ATM signaling pathway. (A and B) ATM bound to HCV NS3-4A. (A) 293FT cells were transfected with 4 μg of pCX4bsr/NS3-4A (O), 4 μg of pCX4bsr/NS3 (O), or 4 μg of pcDNA3-FLAG-ATMwt. The cell lysates of expressed FLAG-ATM were mixed with lysates expressing either NS3-4A or NS3. The cell lysates were immunoprecipitated with both anti-FLAG (M2) and anti-ATM (2C1) antibodies, followed by immunoblotting analysis using either anti-ATM (2C1) or anti-HCV NS3 antibody. The results of Western blot analysis of 1/10 of the cellular lysates with anti-ATM or anti-NS3 antibody are also shown. (B) 293FT cells were cotransfected with 4 μg of pcDNA3-FLAG-ATMwt and/or 4 μg of pCX4bsr/NS3-4A (O). The cell lysates of expressed FLAG-ATM alone were mixed with the O cell lysates. Immunoprecipitation and Western blot analysis were performed as described in panel A. (C) Chk2 did not bind to NS3-4A. 293FT cells were cotransfected with 4 μg of pcDNA3-HA-Chk2wt and/or 4 μg of pCX4bsr/NS3-4A (O). The cell lysates of expressed HA-Chk2 alone were mixed with the O cell lysates. The cell lysates were immunoprecipitated with anti-HA antibody (3F10), followed by Western blot analysis using either anti-HA (HA-7) or anti-HCV NS3 antibody. The results of Western blot analysis of 1/10 of the cellular lysates with anti-HA or anti-NS3 antibody are also shown. (D) ATM was not cleaved by HCV NS3-4A protease. 293FT cells were cotransfected with 4 μg of pCX4bsr/NS3-4A (O) and/or 4 μg of pcDNA3-FLAG-ATMwt. The results of Western blot analysis of cellular lysates with anti-ATM or anti-NS3 antibody are shown. (E to G) ATM bound to HCV NS5B. (E) The lysates of O or Oc cells were immunoprecipitated with anti-ATM antibody (2C1), followed by immunoblotting analysis using either anti-ATM or anti-HCV NS5B antibody (no. 14). The results of Western blot analysis of 1/10 of the cellular lysates with anti-NS5B antibody are also shown. (F) 293FT cells were cotransfected with 4 μg of pCX4bsr/NS5B (1B-1) and 4 μg of pcDNA3-FLAG-ATMwt. The cell lysates were immunoprecipitated with both anti-FLAG and anti-ATM antibodies, followed by immunoblotting analysis using either anti-ATM or anti-HCV NS5B antibody. (G) Western Blot analysis was performed with anti-NS5B antibody, reusing the same blotted membrane that was used for panel B. (H to J) Chk2 bound to HCV NS5B. (H) 293FT cells were cotransfected with 4 μg of pcDNA3-HA-Chk2wt. The cell lysates of expressed HA-Chk2 were mixed with the O cell lysates and were immunoprecipitated with anti-HA antibody (3F10), followed by immunoblotting analysis using anti-HCV NS5B, anti-HCV NS5A (no. 8926), anti-HCV core protein (CP-9 and CP-11 mixture), or anti-HA (HA-7) antibody. The results of Western blot analysis of 1/10 of the cellular lysates with the same antibodies are also shown. (I) The lysates of O cells were immunoprecipitated with anti-NS5B or anti-Chk2 antibody (DCS-273), followed by immunoblotting analysis using anti-HCV NS5B antibody. The result of Western blot analysis of 1/10 of the cellular lysates with anti-NS5B antibody is also shown. (J) 293FT cells were cotransfected with 4 μg of pCX4bsr/NS5B (1B-1) and 4 μg of pcDNA3-HA-Chk2wt. The cell lysates were immunoprecipitated with anti-HA antibody (3F10), followed by immunoblotting analysis using either anti-HA (HA-7) or anti-HCV NS5B antibody. IP, immunoprecipitation; WB, Western blotting; IgG, immunoglobulin G.

O cells were immunoprecipitated with anti-ATM antibody, and then immunoblotting analysis using either anti-ATM or anti-NS5B antibody was performed. The results revealed that endogenous ATM bound to endogenous NS5B (Fig. 6E). Furthermore, we confirmed that ATM bound to NS5B in immunoprecipitation analysis using lysates from 293FT cells, in which NS5B (1B-1 strain) and FLAG-tagged ATM were overexpressed (Fig. 6F). Similarly, we confirmed that FLAG-tagged ATM bound to NS5B derived from O cell lysates in immunoprecipitation analysis using lysates from 293FT cells in which FLAG-tagged ATM was overexpressed (Fig. 6G). Finally, to determine which HCV protein binds to Chk2, the 293FT cell lysates of overexpressed HA-Chk2 were mixed with the O cell lysates and were immunoprecipitated with anti-HA antibody, followed by Western blot analysis using anti-HCV NS5B, anti-HCV NS5A, anti-HCV core protein, or anti-HA antibody. Consistent with the immunofluorescence result that Chk2 partially colocalized with NS5B (Fig. 5C), we observed that HA-tagged Chk2 bound to NS5B (Fig. 6H). Importantly, we found that endogenous Chk2 bound to endogenous NS5B derived from O cells (Fig. 6I). In addition, HA-tagged Chk2 bound to NS5B in immunoprecipitation analysis using lysates from 293FT cells in which NS5B (1B-1 strain) and HA-tagged Chk2 were overexpressed (Fig. 6J). Thus, Chk2 also interacted with NS5B as well as ATM. Taking these results together, we conclude that HCV targets ATM and Chk2 DNA damage sensors and that the ATM signaling pathway is required for HCV RNA replication.

DISCUSSION

ATM has been implicated as a target of most DNA viruses, harboring their genomes in the form of dsDNA which can activate or inhibit the ATM signaling pathway (17). In this study, we have demonstrated for the first time that the ATM signaling pathway is required for HCV RNA replication even though HCV does not have a dsDNA genome, unlike DNA viruses. In this regard, Machida et al. previously proposed that HCV infection and the expression of HCV NS3 and core protein induced dsDNA breaks (18, 19). Furthermore, NS3 has DNA helicase activity by which it unwinds dsDNA, suggesting that NS3 affects host dsDNA (22, 25). Thus, HCV infection might trigger the activation of ATM without a dsDNA genome. In fact, we observed weak but significant phosphorylation of Chk2 at threonine 68, the specific marker for ATM activation, in the HCV RNA-replicating cells (O and sO cells) but not in the HCV-negative Oc and sOc cells (Fig. 3A), suggesting that the ATM-dependent DNA damage response is constantly stimulated in persistent HCV RNA-replicating cells. Furthermore, we demonstrated that ATM preferentially bound to NS3-4A over NS3 alone (Fig. 5B) and that ATM partially colocalized with NS3-4A in the perinuclear region, where HCV is known to form a replication complex and replicate itself, and in dispersed points throughout the cytoplasm (Fig. 5A), indicating the interaction of ATM with NS3-4A. Interestingly, Lai et al. very recently reported that NS3-4A impaired DNA repair and enhanced sensitivity to ionizing radiation through interaction with ATM (15). However, we observed an equivalent level of Chk2 phosphorylation at threonine 68, a direct downstream target of ATM (20, 21), in both HCV RNA-replicating cells (O cells) and HCV-negative cells (Oc cells) after treatment with adriamycin (Fig. 3A), suggesting that Chk2 phosphorylation by ATM is not impaired by HCV RNA replication. In this regard, Gaspar and Shenk also showed that human cytomegalovirus could inhibit a DNA damage response by mislocalizing ATM and phosphorylated Chk2 at threonine 68 to a cytoplasmic virus assembly zone, indicating that human cytomegalovirus blocked at the level of Chk2 (9). On the other hand, dsDNA triggers IFN immune defenses through retinoic acid-induced gene I, the mitochondrial antiviral signaling protein, or the DNA-dependent activator of IFN-regulatory factor (7, 26); and NS3-4A protease, which is known to cleave the mitochondrial antiviral signaling protein, can block it (26), suggesting that interaction of NS3-4A with ATM is partially involved in such a common antiviral signaling pathway. On the other hand, we previously demonstrated that HCV NS5B-expressing PH5CH8 immortalized human hepatocyte cells were susceptible to DNA damage in the form of dsDNA breaks (23). In this regard, we have found that HCV NS5B could bind to both ATM and Chk2 (Fig. 5B and C and 6E to J). Together, these results indicate that HCV might hijack ATM and Chk2 and utilize ATM and Chk2 for HCV RNA replication, thereby resulting in impairment of DNA repair, enhancement of mutation frequency, and development of hepatocellular carcinoma.

Finally, consistent with our finding that ATM was required for HCV RNA replication, an ATM kinase inhibitor efficiently suppressed genome-length HCV RNA replication at an EC_{50} of approximately 2 μM at 72 h after the treatment (Fig. 4A). Similarly, Lau et al. reported that the same ATM kinase inhibitor could suppress HIV-1 replication at an EC_{50} of approximately 2.3 μM (16). Importantly, the EC_{50} for HIV-1 replication is similar to that for HCV replication. Thus, this or other ATM kinase inhibitors may represent a novel approach for the clinical treatment of patients with chronic hepatitis C as well as AIDS patients.

ACKNOWLEDGMENTS

We thank D. Trono, R. Agami, R. Iggo, M. Kastan, S. J. Elledge, M. Kohara, A. Takamizawa, and M. Hijikata for the VSV-G-pseudotyped HIV-1-based vector system (pCMVR8.91 and pMDG2) and for pSUPER, pRDI292, pcDNA3-FLAG-ATM, and pcDNA3-HA-Chk2, and for anti-NS3 antibody, anti-NS5B antibody, anti-NS5A antibody, and 293FT cells. We also thank A. Morishita and T. Nakamura for their technical assistance.

This work was supported by a Grant-in-Aid for Young Scientists (B) from the Ministry of Education, Culture, Sports, Science and Technology (MEXT); by a Grant-in-Aid for Research on Hepatitis from the Ministry of Health, Labor, and Welfare of Japan; by the Ichiro Kanehara Foundation; and by a Research Fellowship from the Japan Society for the Promotion of Science.

REFERENCES

1. **Ariumi, Y., P. Turelli, M. Masutani, and D. Trono.** 2005. DNA damage sensors ATM, ATR, DNA-PKcs, and PARP-1 are dispensable for human immunodeficiency virus type 1 integration. J. Virol. **79:**2973–2978.
2. **Ariumi, Y., and D. Trono.** 2006. Ataxia-telangiectasia-mutated (ATM) protein can enhance human immunodeficiency virus type 1 replication by stimulating Rev. function. J. Virol. **80:**2445–2452.
3. **Ariumi, Y., M. Kuroki, K. Abe, H. Dansako, M. Ikeda, T. Wakita, and N. Kato.** 2007. DDX3 DEAD-box RNA helicase is required for hepatitis C virus RNA replication. J. Virol. **81:**13922–13926.
4. **Bridge, A. J., S. Pebernard, A. Ducraux, A.-L. Nicoulaz, and R. Iggo.** 2003. Induction of an interferon response by RNAi vectors in mammalian cells. Nat. Genet. **34:**263–264.

5. **Brummelkamp, T. R., R. Bernard, and R. Agami.** 2002. A system for stable expression of short interfering RNAs in mammalian cells. Science **296:**550–553.
6. **Canman, C. E., D.-S. Lim, K. A. Cimprich, Y. Taya, K. Tamai, K. Sakaguchi, E. Apella, M. B. Kastan, and J. D. Siliciano.** 1998. Activation of the ATM kinase by ionizing radiation and phosphorylation of p53. Science **281:**1677–1679.
7. **Cheng, G., J. Zhong, J. Chung, and F. V. Chisari.** 2007. Double-stranded DNA and double-stranded RNA induces a common antiviral signaling pathway in human cells. Proc. Natl. Acad. Sci. USA **104:**9035–9040.
8. **Dansako, H., M. Ikeda, and N. Kato.** 2007. Limited suppression of the interferon-beta production by hepatitis C virus serine protease in cultured human hepatocytes. FEBS J. **274:**4161–4176.
9. **Gaspar, M., and T. Shenk.** 2006. Human cytomegalovirus inhibits a DNA damage response by mislocalizing checkpoint proteins. Proc. Natl. Acad. Sci. USA **103:**2821–2826.
10. **Harper, J. W., and S. J. Elledge.** 2007. The DNA damage response: ten years after. Mol. Cell **28:**739–745.
11. **Ikeda, M., K. Abe, H. Dansako, T. Nakamura, K. Naka, and N. Kato.** 2005. Efficient replication of a full-length hepatitis C virus genome, strain O, in cell culture, and development of a luciferase reporter system. Biochem. Biophys. Res. Commun. **329:**1350–1359.
12. **Kato, N., M. Hijikata, Y. Ootsuyama, M. Nakagawa, S. Ohkoshi, T. Sugimura, and K. Shimotohno.** 1990. Molecular cloning of the human hepatitis C virus genome from Japanese patients with non-A, non-B hepatitis. Proc. Natl. Acad. Sci. USA **87:**9524–9528.
13. **Kato, N.** 2001. Molecular virology of hepatitis C virus. Acta Med. Okayama **55:**133–159.
14. **Kato, N., K. Sugiyama, K. Namba, H. Dansako, T. Nakamura, M. Takami, K. Naka, A. Nozaki, and K. Shimotohno.** 2003. Establishment of a hepatitis C virus subgenomic replicon derived from human hepatocytes infected in vitro. Biochem. Biophys. Res. Commun. **306:**756–766.
15. **Lai, C. K., K. S. Jeng, K. Machida, Y. S. Cheng, and M. M. Lai.** 2008. Hepatitis C virus NS3/4A protein interacts with ATM, impairs DNA repair and enhances sensitivity to ionizing radiation. Virology **370:**295–309.
16. **Lau, A., K. M. Swinbank, P. S. Ahmed, D. L. Taylor, S. P. Jackson, G. C. Smith, and M. J. O'Connor.** 2005. Suppression of HIV-1 infection by a small molecule inhibitor of the ATM kinase. Nat. Cell Biol. **7:**493–500.
17. **Lilley, C. E., R. A. Schwartz, and M. D. Weitzman.** 2007. Using or abusing: viruses and the cellular DNA damage response. Trends Microbiol. **15:**119–126.
18. **Machida, K., K. T. Cheng, V. M. Sung, S. Shimodaira, K. L. Lindsay, A. M. Levine, M. Y. Lai, and M. M. Lai.** 2004. Hepatitis C virus induces a mutator phenotype: enhanced mutations of immunoglobulin and protooncogenes. Proc. Natl. Acad. Sci. USA **101:**4262–4267.
19. **Machida, K., K. T. Cheng, V. M. Sung, K. J. Lee, A. M. Levine, and M. M. Lai.** 2004. Hepatitis C virus infection activates the immunologic (type II) isoform of nitric oxide synthase and thereby enhances DNA damage and mutations of cellular genes. J. Virol. **78:**8835–8843.
20. **Matsuoka, S., M. Huang, and S. J. Elledge.** 1998. Linkage of ATM to cell cycle regulation by the Chk2 protein kinase. Science **282:**1893–1897.
21. **Matsuoka, S., G. Rotman, A. Ogawa, Y. Shiloh, K. Tamai, and S. J. Elledge.** 2000. Ataxia telangiectasia-mutated phosphorylates Chk2 in vivo and in vitro. Proc. Natl. Acad. Sci. USA **97:**10389–10394.
22. **Myong, S., M. M. Bruno, A. M. Pyle, and T. Ha.** 2007. Spring-loaded mechanism of DNA unwinding by hepatitis C virus NS3 helicase. Science **317:**513–516.
23. **Naka, K., H. Dansako, N. Kobayashi, M. Ikeda, and N. Kato.** 2006. Hepatitis C virus NS5B delays cell cycle progression by inducing interferon-β via Toll-like receptor 3 signaling pathway without replicating viral genomes. Virology **346:**348–362.
24. **Naldini, L., U. Blömer, P. Gallay, D. Ory, R. Mulligan, F. H. Gage, I. M. Verma, and D. Trono.** 1996. In vivo gene delivery and stable transduction of nondividing cells by a lentiviral vector. Science **272:**263–267.
25. **Pang, P. S., E. Jankowsky, P. J. Planet, and A. M. Pyle.** 2002. The hepatitis C viral NS3 protein is a processive DNA helicase with cofactor enhanced RNA unwinding. EMBO J. **21:**1168–1176.
26. **Takaoka, A., Z. Wang, M. K. Choi, H. Yanai, H. Negishi, T. Ban, Y. Lu, M. Miyagishi, T. Kodama, K. Honda, Y. Ohba, and T. Taniguchi.** 2007. DAI (DLM-1/ZBP1) is a cytosolic DNA sensor and an activator of innate immune response. Nature **448:**501–505.
27. **Tanaka, T., N. Kato, M. J. Cho, and K. Shimotohno.** 1995. A novel sequence found at the 3′ terminus of hepatitis C virus genome. Biochem. Biophys. Res. Commun. **215:**744–749.
28. **Thomas, D. L.** 2000. Hepatitis C epidemiology. Curr. Top. Microbiol. Immunol. **242:**25–41.
29. **Wakita, T., T. Pietschmann, T. Kato, T. Date, M. Miyamoto, Z. Zhao, K. Murthy, A. Habermann, H. G. Kräusslich, M. Mizokami, R. Bartenschlager, and T. J. Liang.** 2005. Production of infectious hepatitis C virus in tissue culture from a cloned viral genome. Nat. Med. **11:**791–796.
30. **Zufferey, R., D. Nagy, R. J. Mandel, L. Naldini, and D. Trono.** 1997. Multiply attenuated lentiviral vector achieves efficient gene delivery in vivo. Nat. Biotechnol. **15:**871–875.

Virus Research 137 (2008) 72–79

Contents lists available at ScienceDirect

Virus Research

journal homepage: www.elsevier.com/locate/virusres

A new living cell-based assay system for monitoring genome-length hepatitis C virus RNA replication

Hiromichi Dansako, Masanori Ikeda, Ken-ichi Abe, Kyoko Mori, Kazunori Takemoto, Yasuo Ariumi, Nobuyuki Kato*

Department of Molecular Biology, Okayama University Graduate School of Medicine, Dentistry, and Pharmaceutical Sciences, 2-5-1 Shikata-cho, Okayama 700-8558, Japan

ARTICLE INFO

Article history:
Received 22 February 2008
Received in revised form 6 June 2008
Accepted 6 June 2008
Available online 21 July 2008

Keywords:
Hepatitis C virus
Genome-length HCV RNA
Living cell-based assay
Green fluorescent protein
OGF7 assay system
Anti-HCV reagents

ABSTRACT

We previously developed a cell-based luciferase reporter assay system for monitoring genome-length hepatitis C virus (HCV) RNA replication (OR6 assay system). Here, we aimed to develop a new living cell-based reporter assay system using enhanced green fluorescent protein (EGFP). Genome-length HCV RNAs encoding EGFP were introduced into a subline of HuH-7 cells and G418 selection was performed. One cloned cell line, OGF7, was successfully selected from among the several G418-resistant cell lines obtained, and the robust expression of HCV RNA and proteins in OGF7 cells was confirmed. The fluorescent intensity of OGF7 cells was decreased by interferon-α treatment in a dose-dependent manner, and it correlated well with the HCV RNA concentration. We demonstrated that the interferon-α sensitivity in the OGF7 assay system measuring the fluorescent intensity was equivalent to that of the OR6 assay system, and that the OGF7 assay system was useful for quantitative evaluation of anti-HCV reagents. The OGF7 assay system is expected to be the most time-saving and inexpensive assay system for high-throughput screening of anti-HCV reagents.

1. Introduction

Persistent hepatitis C virus (HCV) infection frequently causes active liver disease in the form of chronic hepatitis (Choo et al., 1989; Kuo et al., 1989), liver cirrhosis, and hepatocellular carcinoma (Ohkoshi et al., 1990; Saito et al., 1990). HCV infection has now become a serious health problem, with at least 170 million people currently infected worldwide (Thomas, 2000). HCV is an enveloped positive single-stranded RNA (9.6 kb) virus belonging to the *Flaviviridae* (Kato et al., 1990; Tanaka et al., 1995). The HCV genome encodes a large polyprotein precursor of approximately 3000 amino acid (aa) residues, which is cleaved co- and post-translationally into at least 10 proteins in the following order: core, envelope 1 (E1), E2, p7, non-structural protein 2 (NS2), NS3, NS4A, NS4B, NS5A, and NS5B. These cleavages are mediated by the host and virally encoded proteases (Hijikata et al., 1991, 1993; Kato, 2001). NS5B possessing an RNA-dependent RNA polymerase (RdRp) activity is the central enzyme in replication of the HCV genome (Kato, 2001).

In the recent past, interferon (IFN) was used as the main treatment for patients with chronic hepatitis C. Currently, the combination of pegylated-IFN (PEG-IFN) and ribavirin is the standard therapy worldwide, although only 50% of patients show a sustained virological response to this therapy (Hayashi and Takehara, 2006). Several clinical drugs have been proposed as adjuvants to IFN, including cyclosporine A (CsA) (Watashi et al., 2003), mizoribine (Naka et al., 2005), and statins (Ikeda et al., 2006; Ye et al., 2003). Currently, NS3 proteinase/helicase activity and NS5B RdRp activity have been considered as targets for the development of anti-HCV reagents (e.g., the NS3 protease inhibitor BILN 2061 (Lamarre et al., 2003). To date, however, we have not obtained HCV-specific drugs possessing more effective anti-HCV activity than PEG-IFN. Therefore, a more convenient high-throughput screening system is still required to explore more effective anti-HCV reagents.

We previously developed a cell-based genome-length HCV RNA replication system using *Renilla* luciferase as a reporter in order to monitor the HCV RNA replication level (OR6 assay system) (Ikeda et al., 2005; Naka et al., 2005). Other groups have also developed cell-based subgenomic HCV replicon systems using secreted alkaline phosphatase (Yi et al., 2002) or beta-lactamase (Murray et al., 2003) as a reporter. However, these assay systems are still quite time- and cost-intensive methods for measuring enzyme activity.

In the present study, we report a new living cell-based reporter assay system that is able to monitor the level of genome-length HCV RNA replication and to reduce both the time required and the expense.

* Corresponding author. Tel.: +81 86 235 7385; fax: +81 86 235 7392.
E-mail address: nkato@md.okayama-u.ac.jp (N. Kato).

0168-1702/$ – see front matter © 2008 Elsevier B.V. All rights reserved.
doi:10.1016/j.virusres.2008.06.001

2. Materials and methods

2.1. Reagents

IFN-α, IFN-γ, and CsA were purchased from Sigma–Aldrich (St. Louis, MO). IFN-β was a gift from Toray Industries (Tokyo, Japan). Fluvastatin (FLV) was purchased from Calbiochem (San Diego, CA).

2.2. Cell culture

Genome-length HCV RNA replicating cells and OR6c cells were maintained as described previously (Ikeda et al., 2005). OR6c cells are cured OR6 cells (Naka et al., 2005) from which genome-length HCV RNA was eliminated by IFN-α treatment as described previously (Ikeda et al., 2005).

2.3. Construction of plasmids and RNA synthesis

The plasmids used in this study (Fig. 1A and B) were constructed on the basis of the plasmid pON/C-5B/KE (Ikeda et al., 2005). The plasmid pON/C-5B/KE contains neomycin phosphotransferase (Neo^R) downstream of HCV internal ribosome entry site (IRES) and the full-length HCV-O polyprotein-coding sequence downstream of the encephalomyocarditis virus (EMCV) IRES, and K1609E mutation (Ikeda et al., 2005), was introduced into the NS3 helicase region as the adaptive mutation. The plasmid pOGN/C-5B/KE (Fig. 1A(1)) was constructed from the plasmid pON/C-5B/KE by inserting the PCR product of enhanced green fluorescent protein (EGFP; Clontech Laboratories, Inc., Mountain View, CA) into the AscI recognition site of the 5′-end of the Neo^R gene. The plasmids pON/GC-5B/KE (Fig. 1A(2)) and pON/C-5B G2390/KE (Fig. 1A(3)) were constructed from the plasmid pON/C-5B/KE by inserting the PCR product of EGFP into the XhoI recognition site of the 5′-end of the core-coding sequence and at aa position 2390 (Moradpour et al., 2004) in the NS5A-coding sequence, respectively. Both recognition sites were introduced by PCR mutagenesis with primers containing these recognition sites according to the previously described method (Dansako et al., 2005). To construct the plasmids pOGN/C-5B G2390/KE (Fig. 1B(4)) and pON/GC-5B G2390/KE (Fig. 1B(6)), the EcoRI-SpeI fragments of the plasmids pOGN/C-5B/KE and pON/GC-5B/KE, respectively, were replaced with the EcoRI-SpeI region of the plasmid pON/C-5B G2390/KE. The EcoRI recognition site is located at the 5′-end of HCV IRES, and the SpeI recognition site is located at the 5′-end of the NS3 region within the plasmid pON/C-5B/KE, respectively. To construct the plasmids pOGN/GC-5B/KE (Fig. 1B(5)) and pOGN/GC-5B G2390/KE (Fig. 1B(7)), the EcoRI-RsrII fragment of the plasmid pOGN/C-5B/KE was replaced with the EcoRI-RsrII region of the plasmids pON/GC-5B/KE and pON/GC-5B G2390/KE, respectively. The RsrII recognition site is located in the 3′-end of the Neo^R region within the plasmid pON/C-5B/KE. The obtained plasmids were linearized by XbaI and were used for RNA synthesis with T7 MEGAscript (Ambion, Austin, TX) as previously described (Kato et al., 2003).

2.4. RNA transfection and selection of G418-resistant cells

The transfection of genome-length HCV RNA synthesized in vitro into OR6c cells was performed by electroporation, and the cells were selected in the presence of G418 (0.3 mg/ml; Invitrogen) for 3 weeks as described previously (Kato et al., 2003).

2.5. Visualization of the fluorescence by EGFP

The fluorescence of EGFP was directly visualized by a fluorescence microscope (Axiovert 25CFL; Carl Zeiss) or a confocal laser-scanning microscope (LSM510; Carl Zeiss). The cells were fixed with 4% paraformaldehyde and were photographed under a fluorescence microscope or a confocal laser-scanning microscope as described previously (Dansako et al., 2003).

2.6. Integration analysis

Genomic DNA was extracted from the cultured cells by using a DNeasy Blood & Tissue Kit (QIAGEN, Valencia, CA). The HCV 5′-untranslated region (UTR) and the IFN-β gene were detected according to a method described previously (Kato et al., 2003). To test the efficiency of the PCR analysis and the quality of the genomic DNAs, a set of primers was used for the PCR detection of an intronless IFN-β gene (1 copy per haploid genome; the expected PCR product is 341 bp).

2.7. Northern blot analysis

Total RNA was extracted from the cultured cells by using an RNeasy Mini Kit (QIAGEN). HCV RNA and β-actin were detected according to a method described previously (Ikeda et al., 2005).

2.8. Measurement of the fluorescent intensity in living cells replicating a genome-length HCV RNA with EGFP

The cells replicating a genome-length HCV RNA with EGFP (5×10^4) were plated onto 12-well plates. By using a fluorometer (Fluoroskan Ascent; Thermo Fisher Scientific K.K., Yokohama, Japan), the fluorescent intensity in living cells was measured at 24, 48, and 72 h. In several experiments, the fluorescent intensity in living cells was measured only at 72 h after the treatment with reagents. After the measurements of the fluorescent intensity, the cells were subjected to Western blot analysis for HCV proteins and quantitative RT-PCR analysis for HCV RNA.

2.9. Western blot analysis

The preparation of cell lysates, the sodium dodecyl sulfate-polyacrylamide gel electrophoresis, and the immunoblotting analysis were performed as previously described (Hijikata et al., 1993). Production of core, E1, NS3, NS5A, and NS5B proteins in the O and OGF7 cells was analyzed by immunoblotting using anti-core (CP11; Institute of Immunology, Tokyo, Japan), anti-E1 (a generous gift from Dr. M. Kohara, Tokyo Metropolitan Institute of Medical Science), anti-NS3 (Novocastra Laboratories, Newcastle, UK), anti-NS5A (a generous gift from Dr. A. Takamizawa, Research Foundation for Microbial Diseases, Osaka University), and anti-NS5B (a generous gift from Dr. M. Kohara, Tokyo Metropolitan Institute of Medical Science) antibodies, respectively. Production of EGFP-Neo^R fusion protein was also detected by anti-GFP antibody (JL-8; Clontech). β-Actin antibody (AC-15; Sigma) was used as the control for the amount of protein loaded per lane. Immunocomplexes were detected with the Renaissance enhanced chemiluminescence assay (PerkinElmer Life Sciences, Boston, MA).

2.10. Quantitative RT-PCR analysis

The quantitative RT-PCR analysis for HCV RNA was performed by using a real-time LightCycler PCR as described previously (Ikeda et al., 2005).

3. Results

3.1. Establishment of the cloned cell lines replicating a genome-length HCV RNA with EGFP

We previously developed a dicistronic genome-length HCV RNA (O strain of genotype 1b) replication system that stably expresses *Renilla* luciferase as a reporter in order to monitor the level of HCV RNA replication (OR6 assay system) (Ikeda et al., 2005; Naka et al., 2005). To further facilitate mass screening of potential candidates for anti-HCV reagents, we attempted to develop a novel assay system for monitoring the level of HCV RNA replication without lysis of cells. For this purpose, we chose EGFP as a reporter, and we first tried to establish cloned cell lines that efficiently replicate genome-length HCV RNA encoding EGFP. All of the constructed plasmids (Fig. 1) were used as templates for RNA synthesis in vitro, and then the transcribed RNAs were transfected into OR6c cells by the electroporation method, as described in Section 2. After 3 weeks of G418 selection, we obtained several G418-resistant colonies from the OGN/C-5B/KE RNA, ON/GC-5B/KE RNA, ON/C-5B G2390/KE RNA, or OGN/GC-5B/KE RNA-introduced cells, and most of the G418-resistant colonies were successfully established as cell lines (Fig. 1). In contrast, no G418-resistant colonies were obtained from the OGN/C-5B G2390/KE RNA, ON/GC-5B G2390/KE RNA, or OGN/GC-5B G2390/KE RNA-introduced cells (Fig. 1).

To select a cloned cell line showing the highest expression level of EGFP and HCV protein, we first performed Western blot analysis for the detection of EGFP and HCV NS3 protein. The results revealed that OGN/C-5B/KE clone 7, ON/GC-5B/KE clone 3, and OGN/GC-5B/KE clone 3 showed marginally higher expression levels of EGFP and HCV NS3 protein than the other clones (data not shown). Because, in the examination by fluorescence microscopy,

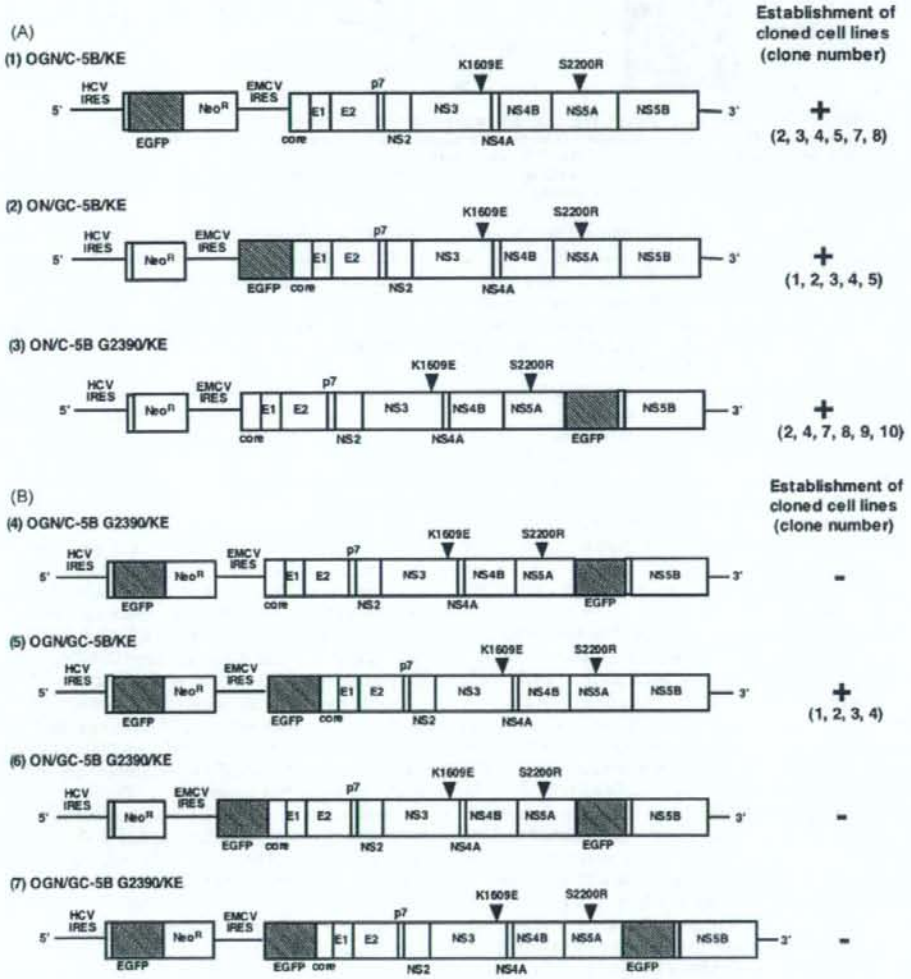

Fig. 1. Schematic presentation of various genome-length HCV RNAs (HCV-O strain) containing an EGFP-encoding sequence. (A) Genome-length HCV RNAs containing one copy of the EGFP-encoding sequence. The basic construct is described in our previous study (Ikeda et al., 2005). The EGFP-encoding region is depicted as a shaded box. Neomycin phosphotransferase is indicated as Neo^R. K1609E and S2200R are adaptive mutations found in previous studies (Ikeda et al., 2005; Kato et al., 2003). (B) Genome-length HCV RNAs containing two or three copies of EGFP-encoding sequence.

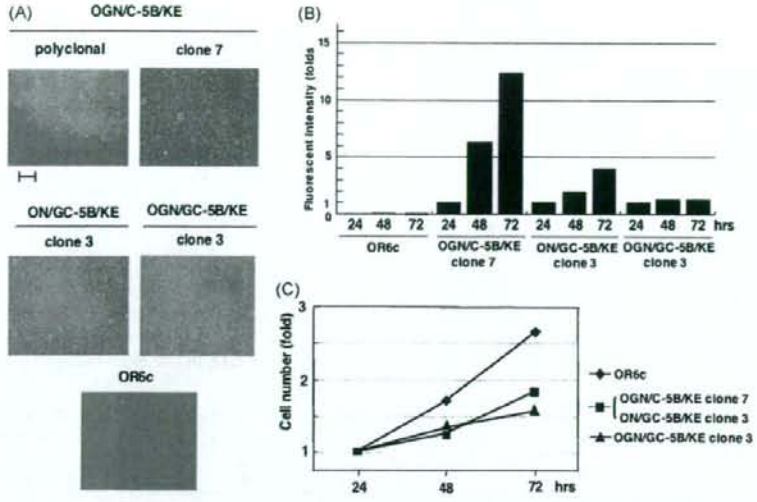

Fig. 2. Fluorescent intensities of G418-resistant cell lines. (A) Visualization of the fluorescence of G418-resistant cell lines under a fluorescence microscope. The panels show the fluorescence of expressed EGFP. Bar, 200 μm. (B) Time course of the fluorescent intensity of G418-resistant cell lines. The fluorescent intensity was measured at 24, 48, and 72 h after cell-seeding by a fluorometer as described in Section 2. For calculating the fluorescent intensity in each cell line, the intensity at 24 h after cell seeding was assigned a value of 1. OR6c cells were used as a negative control. (C) Growth curve of G418-resistant cell lines. The cells were plated onto 6-well plate (1×10^5 cells per well), and the kinetics of cell proliferation during 72 h in culture were determined by Trypan blue treatment. OR6c cells were used as a control.

the fluorescence of EGFP in these selected cell lines was roughly equivalent to that in OGN/C-5B/KE polyclonal cells (Fig. 2A), we next examined the time course of the fluorescent intensities of these cells lines by using a fluorometer, and observed a remarkable, twelve-fold increase in the fluorescent intensity of OGN/C-5B/KE clone 7 cells at 72 h after the start of cell culture in comparison with the intensity at 24 h (Fig. 2B). The fluorescent intensity of ON/GC-5B/KE clone 3 cells was slightly increased at 72 h (approximately four-fold). In contrast to these cell lines, the fluorescent intensity of OGN/GC-5B/KE clone 3 cells did not change during the cell culture. Growth curve analysis of these G418-resistant cell lines revealed that these cell clones had a similar kinetics for cell proliferation, although the growth rate of these cell clones was significantly lower than that of OR6c cells (Fig. 2C). These results suggest that the efficiency of genome-length HCV RNA replication in OGN/C-5B/KE clone 7 cells is higher than that in the other clones. Therefore, we finally selected OGN/C-5B/KE clone 7 (herein designated OGF7) for further characterization.

First, to exclude the possibility that the HCV RNA sequence had become integrated into the genomic DNA, we assayed for the HCV 5′-UTR sequence in the genomic DNA isolated from OGF7 cells by PCR. As a positive control, we used a cloned cell line (Mori et al., 2008) in which the HCV 5′-UTR sequence was integrated into the genomic DNA. The HCV 5′-UTR sequence was not detected in the genomic DNA isolated from OGF7 cells, genome-length HCV RNA-replicating O cells (Ikeda et al., 2005), or OR6c cells (Fig. 3A), although an expected product (266 bp or 205 bp) was detected in the positive control (Fig. 3A, lane PC). These results suggest that the HCV RNA sequence (at least HCV 5′-UTR sequence) is not integrated into the genomic DNA in OGF7 cells. Consistent with these results, an approximately 12 kb RNA of the genome-length HCV RNA encoding EGFP in OGF7 cells was also detected by Northern blot analysis, and its accumulation level was almost the same as that in the O cells (Fig. 3B). In addition, we confirmed by Western blot analysis that OGF7 cells efficiently expressed not only HCV proteins but also the EGFP-Neo^R fused protein, and the expression levels of HCV proteins in the OGF7 cells were also equivalent to those in the O cells (Fig. 3C). In summary, these results indicate that the OGF7 cell line harboring replicative genome-length HCV RNA encoding EGFP as a reporter was stably established.

3.2. *OGF7 living cells are useful for direct monitoring of the level of HCV RNA*

First, we examined whether or not the expression level of EGFP in OGF7 cells was sufficient to allow direct visualization by confocal laser-scanning microscopy. As a consequence, we could detect the fluorescence in addition to the core protein expressed in OGF7 cells (Fig. 4). Furthermore, we confirmed that the detected fluorescence was derived from the EGFP expressed in OGF7 cells, because both the fluorescence and the core protein disappeared after IFN-α treatment (Fig. 4). These results suggest that the replication of genome-length HCV RNA encoding EGFP-Neo^R fused protein occurs efficiently in OGF7 cells. We next examined whether or not the IFN sensitivity of the EGFP level was associated with that of the HCV RNA level in OGF7 cells. The levels of EGFP and HCV RNA were examined by the fluorometer and real-time LightCycler PCR, respectively. The results revealed that the level of reduction in the fluorescent intensity by IFN-α treatment was equivalent to the level of reduction in the HCV RNA level (Fig. 5A and B). In addition, we confirmed by Western blot analysis that the reduction pattern of the EGFP-Neo^R fusion protein by IFN-α treatment was also similar to those of the core and NS3 proteins (Fig. 5C). These results indicate that the expression level of EGFP is sufficient for monitoring of the level of HCV RNA, and suggest that the direct measurement of the fluorescent intensity of the living OGF7 cells was an effective means of monitoring the level of HCV RNA replication.

3.3. *The OGF7 system is useful as a quantitative assay system for various anti-HCV reagents*

To clarify whether or not the OGF7 system is useful as a quantitative antiviral assay system, we first compared the IFN-α sensitivity of the OGF7 fluorescent reporter system with that

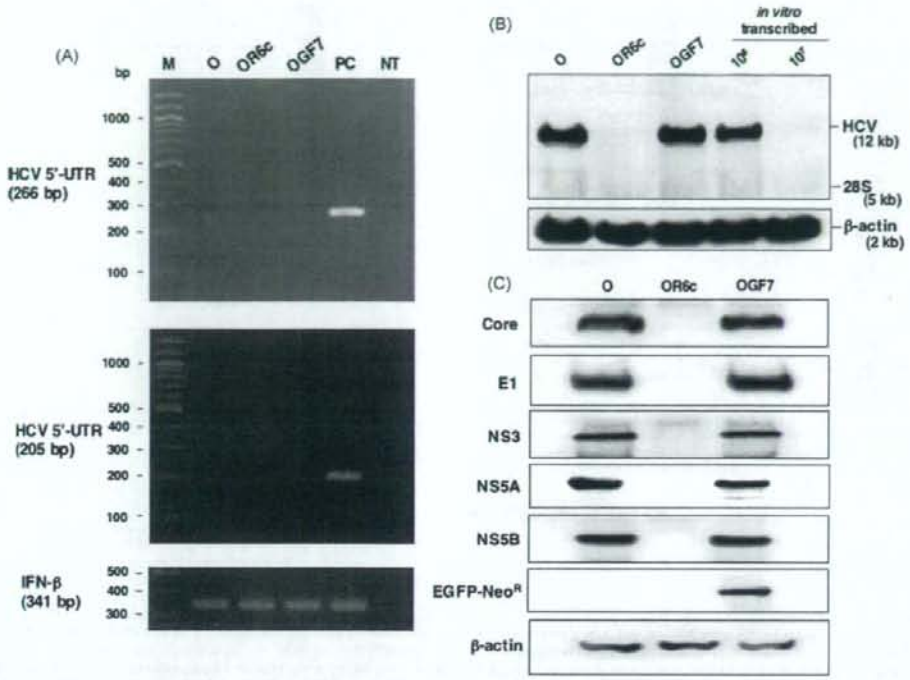

Fig. 3. Characterization of OGF7 cells replicating genome-length HCV RNA encoding EGFP as a reporter. Genome-length HCV RNA-replicating O cells (Ikeda et al., 2005) and OR6c cells (cured OR6 cells) were used for the comparison. (A) HCV genome-derived sequences were not integrated into the genomic DNA from OGF7 cells. Genomic DNA from the OGF7 cells was subjected to PCR for the detection of the HCV 5′-UTR and the IFN-β gene. Genomic DNAs from the O and OR6c cells were also used as negative controls. As a positive control, we used genomic DNA from a cell line (Mori et al., 2008) into which the HCV 5′-UTR sequence had been accidentally integrated (lane PC). PCR without genomic DNA was also performed (lane NT). PCR products (266 and 205 bp for HCV 5′-UTR, or 341 bp for the IFN-β gene) were detected by staining with ethidium bromide after 3% agarose gel electrophoresis. The 100 bp DNA ladder was used as a size marker (lane M). (B) Northern blot analysis. Total RNAs (3 μg each) from the O, OR6c, and OGF7 cells were analyzed by Northern blot analysis using a positive-stranded HCV genome-specific RNA probe (upper panel) and a β-actin-specific RNA probe (lower panel), respectively. In vitro-synthesized ORN/C-5B/KE (Ikeda et al., 2005) RNA (10^7 and 10^8 genome equivalents spiked into normal cellular RNA) was used for the comparison of expression levels. (C) Western blot analysis. Production of core, E1, NS3, NS5A, and NS5B proteins in the O and OGF7 cells was analyzed by immunoblotting using anti-core, anti-E1, anti-NS3, anti-NS5A, and anti-NS5B antibodies, respectively. Production of EGFP-Neo^R fusion protein and β-actin was also detected by anti-GFP and anti-β-actin antibodies, respectively.

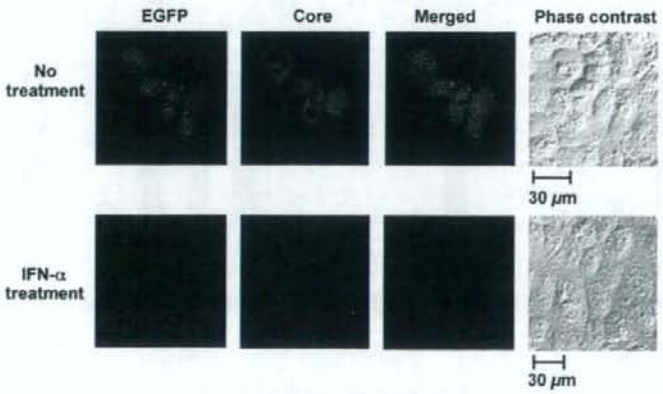

Fig. 4. The EGFP and core protein expressed in OGF7 cells disappeared following IFN-α treatment. OGF7 cells were examined by confocal laser-scanning microscopy. Cells were treated with IFN-α (500 IU/ml for 6 h). The cells were visualized with a fluorescence microscope, and then the cells were stained with anti-core antibody (CP11; Institute of Immunology, Tokyo, Japan) and Cy3-conjugated anti-mouse secondary antibody (Jackson Immuno Research, West Grove, PA) according to a method described previously (Naka et al., 2006). The merged panels show the two-color overlay images. Bar, 30 μm.

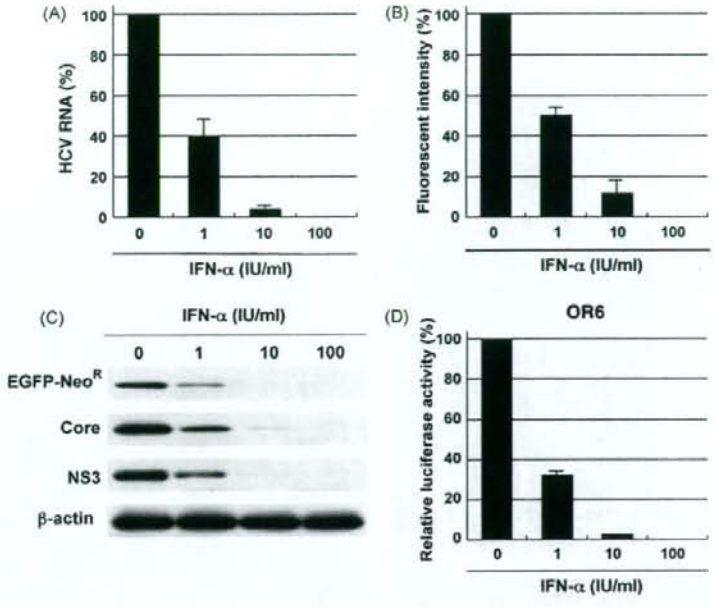

Fig. 5. Effect of IFN-α on genome-length HCV RNA replication in OGF7 and OR6 cells. OGF7 and OR6 cells were treated with IFN-α (0, 1, 10, and 100 IU/ml) for 72 h. After the measurements of the fluorescent intensity of OGF7 cells, the cells were subjected to quantitative RT-PCR analysis for HCV RNA and Western blot analysis. (A) Quantitative RT-PCR analysis of HCV RNA in OGF7 cells. Total RNA extracted from the cells was subjected to real-time LightCycler PCR analysis. The relative level of HCV RNA (%) calculated at each point, when the level of HCV RNA in untreated cells was assigned a value of 100%, is shown here. The experiments were performed in at least triplicate. (B) Fluorescent intensity of OGF7 cells. The fluorometer was used for the measurement of the fluorescent intensity of OGF7 cells. The relative level of the fluorescent intensity calculated, when the fluorescent intensity of untreated cells was taken as 100%, is shown here. The data indicate means from triplicate experiments. (C) Western blot analysis. The production of EGFP-Neo^R, core, and NS3 in OGF7 cells was analyzed by immunoblotting using anti-EGFP, anti-core, and anti-NS3 antibodies, respectively. β-Actin was used as a control for the amount of protein loaded per lane. (D) Renilla luciferase reporter assay using OR6 cells. The relative level of the luciferase activity calculated, when the luciferase activity of untreated cells was assigned a value of 100%, is shown here. The experiments were performed in at least triplicate.

of the OR6 luciferase reporter system. The results revealed that the profile of IFN-α sensitivity obtained by the OGF7 fluorescent system (Fig. 5B) was similar to that obtained using the OR6 luciferase system (Fig. 5D). Although the OGF7 system was slightly less sensitive than the OR6 system, the small difference may have been due to the different cell clones used. Because the results suggested that the OGF7 system is useful as a quantitative antiviral assay system, we proceeded to examine the activities of other anti-HCV reagents using the OGF7 system. The results revealed that the fluorescent intensity of OGF7 cells was decreased by the treatments of IFN-β, IFN-γ, CsA, and FLV in a dose-dependent manner (Fig. 6A), and that the level of the EGFP-Neo^R fusion protein was also decreased by these anti-HCV reagents in a dose-dependent manner (Fig. 6B). These results suggest that the OGF7 system is useful as a quantitative anti-HCV assay system.

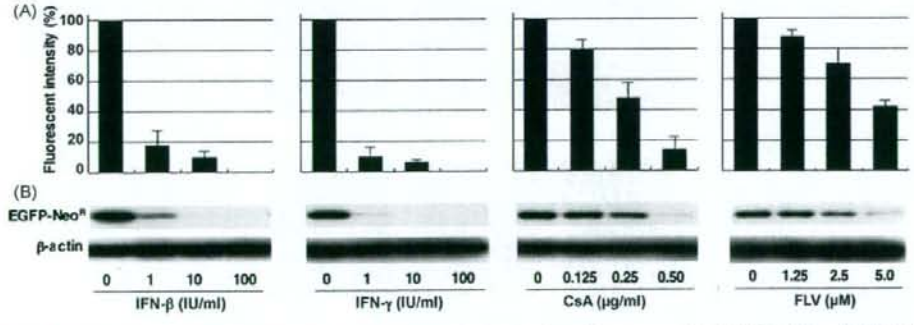

Fig. 6. Effects of IFN-β, IFN-γ, CsA, and FLV on genome-length HCV RNA replication in OGF7 cells. OGF7 cells were treated with IFN-β (0, 1, 10, and 100 IU/ml), IFN-γ (0, 1, 10, and 100 IU/ml), CsA (0, 0.125, 0.25, and 0.5 μg/ml) and FLV (0, 1.25, 2.5, and 5.0 μM). (A) Fluorescent intensity of OGF7 cells. After 72 h of treatment, the fluorescent intensity of OGF7 cells was measured by a fluorometer. The relative level of the fluorescent intensity calculated, when the fluorescent intensity of untreated cells was assigned a value of 100%, is shown here. The data indicate means from triplicate experiments. (B) Western blot analysis. The production level of EGFP-Neo^R was analyzed by immunoblotting using anti-EGFP antibody. β-Actin was used as a control for the amount of protein loaded per lane.

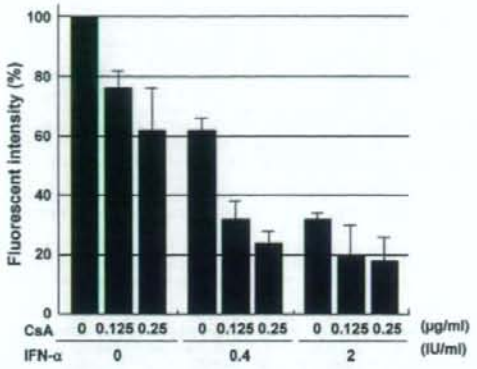

Fig. 7. Effect of IFN-α in combination with CsA on genome-length HCV RNA replication in OGF7 cells. OGF7 cells were co-treated with IFN-α (0, 0.4, and 2.0 IU/ml) and CsA (0, 0.125, and 0.25 μg/ml), and at 72 h after treatment, the fluorescent intensity of OGF7 cells was measured by a fluorometer. The relative level of the fluorescent intensity calculated, when the fluorescent intensity of untreated cells was taken as 100%, is shown here. The data indicate means from triplicate experiments.

3.4. The OGF7 assay system is also useful as a system for evaluating the efficacy of co-treatment with various anti-HCV reagents

Since we demonstrated that the OGF7 system could be used effectively as either a quantitative anti-HCV assay system or OR6 assay system, we further examined whether or not the OGF7 system could be used to evaluate the efficacy of co-treatment with various anti-HCV reagents. The results showed that co-treatment with IFN-α and CsA was more effective than treatment with IFN-α alone (Fig. 7).

Together, the above results led us to conclude that the OGF7 living cell system is the most time-saving and low-cost anti-HCV assay system currently available.

4. Discussion

In the present study, we developed a new living cell-based reporter assay system (OGF7 assay system) for monitoring HCV RNA replication. We demonstrated that this OGF7 assay system was useful for the quantitative evaluation of anti-HCV reagents. Our study suggests that this new assay system is the most time-saving and inexpensive assay system for high-throughput screening of anti-HCV reagents.

To date, several cloned cell lines harboring HCV RNA (Con1 strain of genotype 1b) with EGFP have been reported (Liu et al., 2006; McCormick et al., 2006; Moradpour et al., 2004). However, regarding the Con1 strain, established cell lines are limited to the subgenomic replicon RNA, although several cloned cell lines harboring genome-length HCV RNA (JFH-1 strain of genotype 2a) with EGFP have been recently reported (Kim et al., 2007; Jones et al., 2007; Schaller et al., 2007). Since a quantitative reporter assay system for monitoring the level of HCV RNA replication has not been developed in these studies, we have tried to establish cell lines in which a genome-length HCV RNA encoding two or three copies of EGFP is efficiently replicating. However, from this study we have learned the limitation of RNA genome size. Although we tested seven different kinds of constructs for HCV RNA replication, most of the G418-resistant colonies were obtained from one copy type of EGFP (RNA genome size 11.8 kb) (Fig. 1). Although we obtained G418-resistant colonies from only OGN/GC-5B/KE construct containing two copies of EGFP (RNA genome size 12.5 kb), the fluorescent intensities of these colonies did not increase in a culture time-dependent manner, suggesting that the HCV RNA replication is not efficient in these cloned cells. These findings suggest that the genome size limitation in HCV RNA replication is approximately 12 kb. This suggestion is consistent with the previous finding (Ikeda et al., 2005) obtained in the process of development of the OR6 assay system. However, specific combination (Q1112R and K1609E) of adaptive NS3 mutations, which drastically enhanced the efficiency of genome-length HCV RNA replication (Abe et al., 2007), may overcome the genome size limitation (approximately 12 kb) in HCV RNA replication. When this genome size limitation is solved, a new cell line in which a genome-length HCV RNA encoding both EGFP-Neo^R fused protein and another fluorescent reporter (e.g., EYFP)-NS5A fused protein replicate efficiently may be developed. Such a system would allow us to monitor the levels of HCV RNA and HCV proteins simultaneously.

We demonstrated that the established OGF7 cells were useful as a quantitative antiviral assay system (OGF7 assay system), because the anti-HCV activities of IFN-α, IFN-β, IFN-γ, CsA, and FLV were clearly shown in a dose-dependent manner just as in the evaluation using the OR6 assay system (Ikeda et al., 2005, 2006; Naka et al., 2005; Yano et al., 2007). Furthermore, since the OGF7 assay system allows us to measure, at different times, the same well containing OGF7 cells treated with the reagent, the OGF7 assay system can be considered superior to the OR6 assay system. Finally, since the OGF7 assay system is based on the simple measurement of the fluorescent intensity of living cells, this system has great advantages regarding time and cost for the antiviral assay of a number of reagents. Therefore, the OGF7 assay system is the most convenient method for high-throughput mass screening of a large compound library. Although we used 12-well plates for the assay in this study, we confirmed that we could monitor the level of HCV RNA replication on 24-well plates (data not shown). If the replication level of HCV RNA were to become higher than that in OGF7 cells due to additional adaptive mutation(s), such system might be capable of monitoring the replication level of HCV RNA in the living cells on 48- or 96-well plates. Such a system containing an OGF7 assay could be used to identify more effective and specific anti-HCV reagents in the future.

Acknowledgements

We would like to thank T. Maeta and T. Nakamura for their helpful assistance with the experiments. This work was supported by grants-in-aid for a third-term comprehensive 10-year strategy for cancer control, and for research on hepatitis from the Ministry of Health, Labor, and Welfare of Japan. K.A. was supported by a Research Fellowship from the Japan Society for the Promotion of Science (JSPS) for Young Scientists.

References

Abe, K., Ikeda, M., Dansako, H., Naka, K., Kato, N., 2007. Cell culture-adaptive NS3 mutations required for the robust replication of genome-length hepatitis C virus RNA. Virus Res. 125, 88–97.

Choo, Q.L., Kuo, G., Weiner, A.J., Overby, L.R., Bradley, D.W., Houghton, M., 1989. Isolation of a cDNA clone derived from a blood-borne non-A, non-B viral hepatitis genome. Science 244, 359–362.

Dansako, H., Naganuma, A., Nakamura, T., Ikeda, F., Nozaki, A., Kato, N., 2003. Differential activation of interferon-inducible genes by hepatitis C virus core protein mediated by the interferon stimulated response elements. Virus Res. 97, 17–30.

Dansako, H., Naka, K., Ikeda, M., Kato, N., 2005. Hepatitis C virus proteins exhibit conflicting effects on the interferon system in human hepatocyte cells. Biochem. Biophys. Res. Commun. 336, 458–468.

Hayashi, N., Takehara, T., 2006. Antiviral therapy for chronic hepatitis C: past, present, and future. J. Gastroenterol. 41, 17–27.